https://ntrs.nasa.gov/search.jsp?R=19680010356 2020-03-12T08:45:42+00:00Z

Technical Report No. 1

SPECIAL STUDIES OF AROD SYSTEMS CONCEPTS AND DESIGNS

Contract NAS8-20128

January 15, 1967

Prepared for

National Aeronautics and Space Administration
George C. Marshall Space Flight Center
Huntsville, Alabama 35812

Authors

Dr. E.J. Baghdady
K.W. Kruse
S.A. Meer

Approved by Elie J. Baghdady
Elie J. Baghdady
Technical Director

Submitted by

ADCOM, Inc.
808 Memorial Drive
Cambridge, Massachusetts 02139

TABLE OF CONTENTS

LIST OF ILLUSTRATIONS

LIST OF ILLUSTRATIONS (Cont'd)

1. INTRODUCTION

1.1 General Information

This document constitutes the First Technical Report submitted by ADCOM, Inc. to the George C. Marshall Space Flight Center of the National Aeronautics and Space Administration under Contract NAS 8-20128. The program is concerned with analytical studies, investigations and evaluations relating to the Concept, Design and Tests of the AROD System. This report covers work performed by ADCOM, Inc., in cooperation with and under the technical direction of the Astrionics Laboratory, MSFC with Mr. G. H. Saunders acting as project manager.

In accordance with the overall technical plan of the program, the main objectives of the work covered in this report have been to provide analytical evaluations and studies in support of the AROD development effort under way of Motorola, Inc. Accordingly, this report deals with certain aspects of the system analysis and models presented by Motorola, Inc., in their reports on the AROD system, and presents further investigations of a number of critical system areas.

The Motorola documents[1,2] that have served as a major source of the information utilized in this report are:

> Motorola Inc., Military Electronics Division, "AROD System Description," Report No. 3065-2-1, Prepared for MSFC, Contract No. NAS8-11835, Revisions 1, 2, 3, 4 from 4 June 1965 to 1 March 1966.
>
> Kline, A.J., "AROD Vehicle Tracking Receiver Design," Technical Memorandum No. 3065-26, Government Electronics Division, Aerospace Center, Motorola, Inc., 3 August 1966.

1.2 Summary of Contents

The second section of this report contains computations of signal and noise levels in the AROD system. The necessary system parameters such as noise temperatures and antenna gains, etc., are explicitly noted and the expressions for computation of the signal and noise levels are given. The signal-to- noise ratios are presented for the Vehicle Tracking Receiver, the Station Control Receiver and its Data Demodulator, at all important locations in these systems. The computations show that the system has sufficient signal-to-noise ratio margin at the maximum range of 2000 km.

Section 3 includes various analyses of the performance of the VTR carrier loop. In Sec. 3.2 the carrier loop model is derived and shown to be similar to a second-order phase-locked loop with different ac and dc gains. In Sec. 3.3 the design relations and performance of an RC-integrator type memory are studied. Finally, Sec. 3.4 covers the effects of switching of the S-band transponder antenna on the VTR. This switching of the antenna causes amplitude and phase steps on the uplink S-band signal. The phase error in the VTR carrier loop due to these effects is obtained.

The range loop performance analyses are contained in Sec. 4. In Sec. 4.2 the effect of uplink data on L-code acquisition is investigated. It is shown in this section that the uplink data can reduce the correlation level of the code nearly 25%. This means that uplink data reduces the system threshold during acquisition. In Sec. 4.3 the combined carrier and range processing scheme used in AROD is analyzed. First the basic model of the processing used in AROD is derived, and next expressions for variance of the range-measurement noise are obtained. Also derived is an analytical expression showing the bandwidth advantage of the range loop with and without rate aiding.

Section 5 is a noise analysis of the coherent AGC for the VTR carrier loop IF amplifier. An estimate of the amplitude jitter resulting from input noise is presented. This analysis takes into account both the phase error due to noise in the carrier loop and the nonlinear transformation of the Gaussian IF noise by the AGC amplifier.

2. SIGNAL AND NOISE LEVELS IN THE AROD SYSTEM

2.1 Introduction

This section is simply a computation of the signal-to-noise ratios in the various points of the AROD system that are of interest in the following studies of subsystem performance. Another object of this section was a verification of similar computations by Motorola and identification of their assumptions. Thus the signal-to-noise ratios are presented for the Vehicle Tracking Receiver (VTR), the Station Control Receiver (SCR) and its Data Demodulator. The SNR's are computed at important locations in these subsystems for the several different ranges from 12 km to 37,150 km for the VTR, and from 100 km to 20,000 km for the SCR. Although the AROD system is supposed to be employed mainly within the ranges 100 km to 2,000 km, the ranges outside this region are considered to show the system's ultimate capability for the specified front-end dynamic range of the receiver (-65 dBm to -135 dBm).

2.2 Method of Computation

The following expression gives the total operating noise temperature referred to the receiver input

$$T_{op} = \frac{T_A}{L} + \frac{T_S}{L} + \left(1 - \frac{1}{L}\right)290 + T_R \ ^{o}K \qquad (2.1)$$

where

T_A = Antenna temp in ^{o}K including minor lobe temp and i^2R losses.

T_S = Source temp in ^{o}K.

T_R = Receiver temp in ^oK

= $\left(N.F. - 1\right) 290^o$, N.F. = Noise figure of receiver.

L = Receiving circuit loss ratio.

The input noise power spectral density is then

$$\Phi = 10 \log k\ T_{op}\ \text{dBm/Hz} \qquad (2.2)$$

where $k = 1.38 \times 10^{-20}$. The corresponding noise power in a given bandwidth B in Hz is simply

$$N = 10 \log k\ T_{op}\ B\ \text{dBm} \qquad (2.3)$$

The computation of the signal power is made at the same point in the receiver where the above noise is computed. Let P be the total transmitted power, then received signal power S is

$$S = P + L_T + L_R + L_S + L_P + G\ \text{dB} \qquad (2.4)$$

where

L_T - Transmitter circuit loss and pointing loss for directional antenna.

L_R - Receiver circuit loss and pointing loss

L_S - Free space loss - this loss is a function of frequency and range. If the range is R in kilometers and the carrier frequency is f in megahertz, the loss is

$$L_S = -20 \log (Rf) - 32.45\ \text{dB} \qquad (2.5)$$

L_P - This loss is a function of the transmitting and receiving antennas axial ratios R_T and R_R. The loss is

$$L_P = \frac{P_{min} + P_{max}}{2} \quad dB \tag{2.6}$$

where

$$P_{min} = 10 \log \frac{\left(R_T^2 + 1\right)\left(R_R^2 + 1\right)}{\left(R_T R_R \pm 1\right)^2} \tag{2.7}$$

$$P_{max} = 10 \log \frac{\left(R_T^2 + 1\right)\left(R_R^2 + 1\right)}{\left(R_T \pm R_R\right)^2} \tag{2.8}$$

The plus sign is used when the direction of polarization of both antennas is the same, and minus when opposite.

G - Total transmitter and receiver antenna gains.

$$G = G_T + G_R \quad dB \tag{2.9}$$

We have presented above the most detailed expression for computation of signal and noise levels. Unfortunately, at present the exact size of some of these terms is not known, so that in the following computation we will have to use estimated values. The above expressions will be useful, however, when more complete information is available.

2.3 Signal and Noise Levels in VTR

The input noise density Φ is computed on the basis of the following data

$$\left.\begin{aligned} &T_A = 0\ , \quad T_S = 0 \\ &\text{Noise figure in dB} = 6.5\ \text{dB} \\ &\text{Incidental loss } L = 4 \text{ to } 8\ \text{dB} \end{aligned}\right\} \tag{2.10}$$

Thus

$$T_R = 3.47 \times 290 = 1{,}006^{\circ}\,K$$

while for the two different incidental losses

$$\left(1 - \frac{1}{L}\right) 290 = 174^{\circ}K \quad \text{for} \quad L = 4\ \text{dB}$$
$$= 273^{\circ}K \quad \text{for} \quad L = 8\ \text{dB}$$

the corresponding T_{op} are

$$T_{op} = 1180^{\circ}K \quad \text{for} \quad L = 4\ \text{dB} \tag{2.11a}$$
$$= 1279^{\circ}K \quad \text{for} \quad L = 8\ \text{dB} \tag{2.11b}$$

and the noise density is

$$\Phi = -167.88\ \text{dBm/Hz} \quad \text{for} \quad L = 4\ \text{dB} \tag{2.12a}$$
$$= -167.54\ \text{dBm/Hz} \quad \text{for} \quad L = 8\ \text{dB} \tag{2.12b}$$

To compute the received signal level we have the following information:

$$P = 20\ \text{watts} = 43\ \text{dBm} \tag{2.13}$$

$$\text{total loss} = L_T + L_R + L_P = -8\ \text{dB} \tag{2.14}$$

$$\left.\begin{aligned} &\text{frequency} = 1800\ \text{MHz} \\ &\text{transmitting antenna gain} = G_T = 16\ \text{dB} \\ &\text{receiving antenna gain} = G_R = 3\ \text{dB} \end{aligned}\right\} \tag{2.15}$$

The space loss L_S is a function of range, for example for R = 100 km

$$L_S = -20 \log (100 \times 1800) - 32.45$$
$$= -137.55 \text{ dB} \qquad (2.16)$$

and for every increase in range of 10 the space loss decreases 20 dB. Thus at 100 km the received signal power is

$$S_2 = 43 - 137.55 + 19 - 8$$
$$= -83.6 \text{ dBm} \qquad (2.17a)$$

The values of S at other ranges are as follows:

$S_1 = -65$ dBm at 11.75 km (2.17b)
$S_3 = -109.6$ dBm at 2,000 km (2.17c)
$S_4 = -129.6$ dBm at 20,000 km (2.17d)
$S_5 = -135$ dBm at 37,150 km (2.17e)

Using these signal and noise levels at the VTR input, corresponding signal and noise levels are computed for various locations in the VTR. The computations results are shown directly on the block diagrams of the VTR Multichannel Subsystem and the VTR Tracking Subsection in Figs. 2.1 and 2.2. The value of Φ for these figures corresponds to incidental loss L = -8 dB.

In Fig. 2.2 the signal-to-noise (S/N) ratio in the IF preceding the carrier loop is given as $(S/N)^{IV}$. The corresponding $(S/N)^c$ in the carrier loop bandwidth is given by

$$(S/N)^c = \left(\frac{S}{N}\right)^{IV} \left(\frac{B_{IF}}{B_c^a}\right) \quad \text{in acquisition} \qquad (2.18a)$$

$$= \left(\frac{S}{N}\right)^{IV} \left(\frac{B_{IF}}{4B_c^t}\right) \quad \text{in tracking} \qquad (2.18b)$$

where B_{IF} is the IF bandwidth in Hz and B_c^a and B_c^t are the <u>one-sided</u> loop noise bandwidth in Hz, for acquisition and tracking respectively. The factor

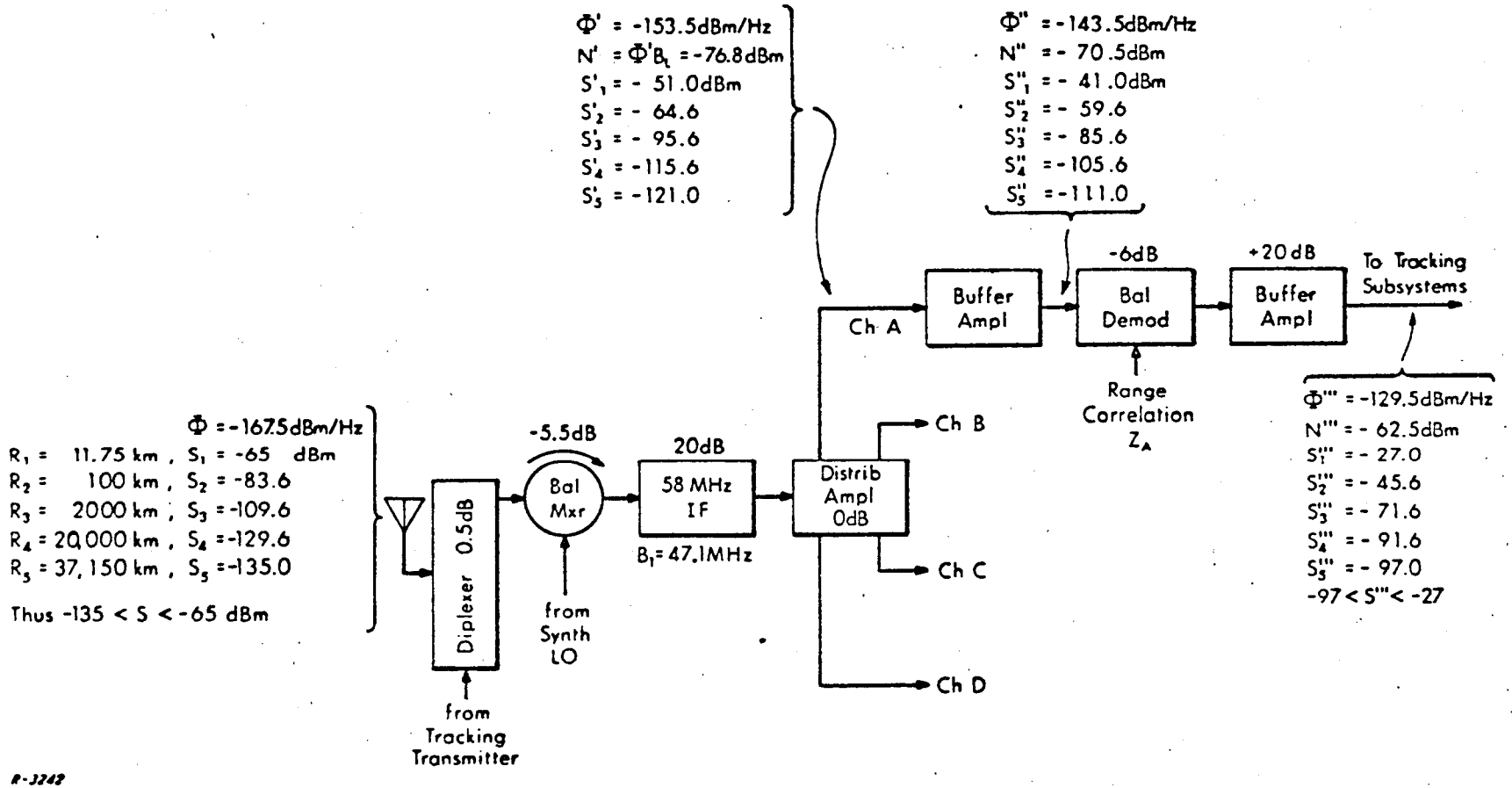

Fig. 2.1 Signal and Noise Levels in Multichannel Subsystem of VTR. (Part of Fig. 4-8, Ref. 1)

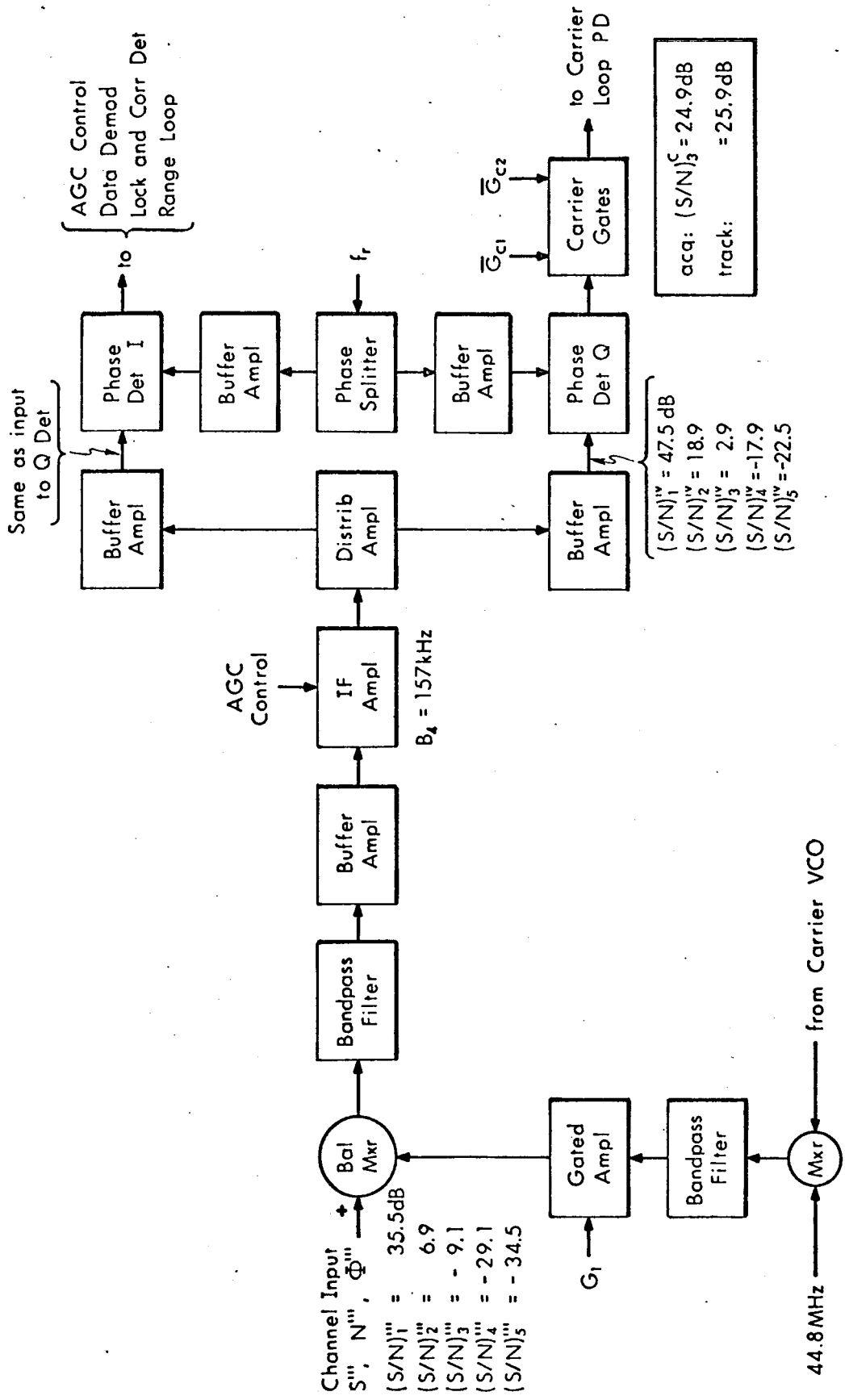

Fig. 2.2 Signal and Noise Levels in VTR Tracking Subsection.
(Part of Fig. 4-11, Ref. 1)

of four is due to the type of switching arrangement employed in the carrier loop.[1] Thus, at the maximum specified range of 2,000 km,

$$(S/N)^c = 24.9 \text{ dB} \quad \text{in acquisition} \tag{2.19a}$$

$$= 25.9 \text{ dB} \quad \text{in tracking} \tag{2.19b}$$

where $B_{IF} = 1.57 \times 10^5$ Hz, $B_c^a = 1000$ Hz and $B_c^t = 200$ Hz. Using one definition of threshold[3] a $(S/N)_T^c = 3.2$ dB we see that the carrier loop has a sufficient margin of operation at maximum range.

2.4 Signal and Noise Levels in the Station Control Receiver

There is little information available on the station control receiver so that we have had to make some estimates of the various terms. The input noise density Φ is computed on the basis of the following values

$$\left.\begin{aligned} T_A &= 30^\circ K && \text{(estimated)} \\ T_S &= 600^\circ && (\quad " \quad) \\ T_R &= 1540^\circ && \text{(N. F. = 8 dB)} \\ L &= 2 \text{ dB} && \text{(estimated)} \end{aligned}\right\} \tag{2.20}$$

Using Eq. (2.1)

$$T_{op} = 2054^\circ K \tag{2.21}$$

The estimated values of T_A and T_S could be considerably higher, on the other hand it is likely that the receiver noise figure may be lower than the specifications. The corresponding noise density is

$$\Phi = -165.6 \text{ dBm} \tag{2.22}$$

The received signal level is computed from the data

$$\left.\begin{aligned} P &= 6 \text{ watts} = 37.8 \text{ dBm} \\ \text{Total losses} &= -4.0 \text{ dB} \\ G_R &= 3.0 \text{ dB} \\ G_T &= 3.0 \text{ dB} \\ f &= 138 \text{ MHz} \end{aligned}\right\} \tag{2.23}$$

For propagation loss taking the range of 100 km for an example

$$L_S = -20 \log 1.38 - 112.5 = -115.3 \text{ dB} \tag{2.24}$$

Hence the received signal power at 100 km is

$$\begin{aligned} S_1 &= 37.8 - 4 + 6 - 115.3 \\ &= -75.5 \text{ dBm} \end{aligned} \tag{2.25}$$

The signal levels for other ranges are tabulated on Fig. 2.3 which is a block diagram of the Station Control Receiver. The resulting signal-to-noise ratios in the following parts of the system are also tabulated. In Fig. 2.4 the corresponding signal-to-noise ratios in the data demodulator are presented.

At the maximum specified range of 2,000 km the carrier, subcarrier and the sub-bit sync loops have the following signal-to-noise ratios in their loop bandwidths

$$(S/N)^c = \left(\frac{S}{N}\right)_2' \left(\frac{150 \times 10^3}{2 \times 10^3}\right) J_o^2(1.2)$$

$$= 28.2 \text{ dB} \quad \text{carrier loop} \tag{2.26}$$

$$(S/N)^{sc} = \left(\frac{S}{N}\right)_2'' \left(\frac{26 \times 10^3}{50}\right) J_1^2(1.2)$$

$$= 45.4 \text{ dB} \quad \text{subcarrier loop} \tag{2.27}$$

$$(S/N)^{sb} = \left(\frac{S}{N}\right)_2'' \left(\frac{26 \times 10^3}{20}\right) J_1^2(1.0)$$

$$= 48.5 \text{ dB} \quad \text{sub-bit sync loop} \tag{2.28}$$

where 1.2 rad is the modulation index of the subcarrier and 1.0 rad is the modulation index of the sub-bit sync subcarrier. It is assumed that the two subcarriers will not be present simultaneously. *

---

* These numbers are obtained from Motorola specifications on the Station Control Transmitter.

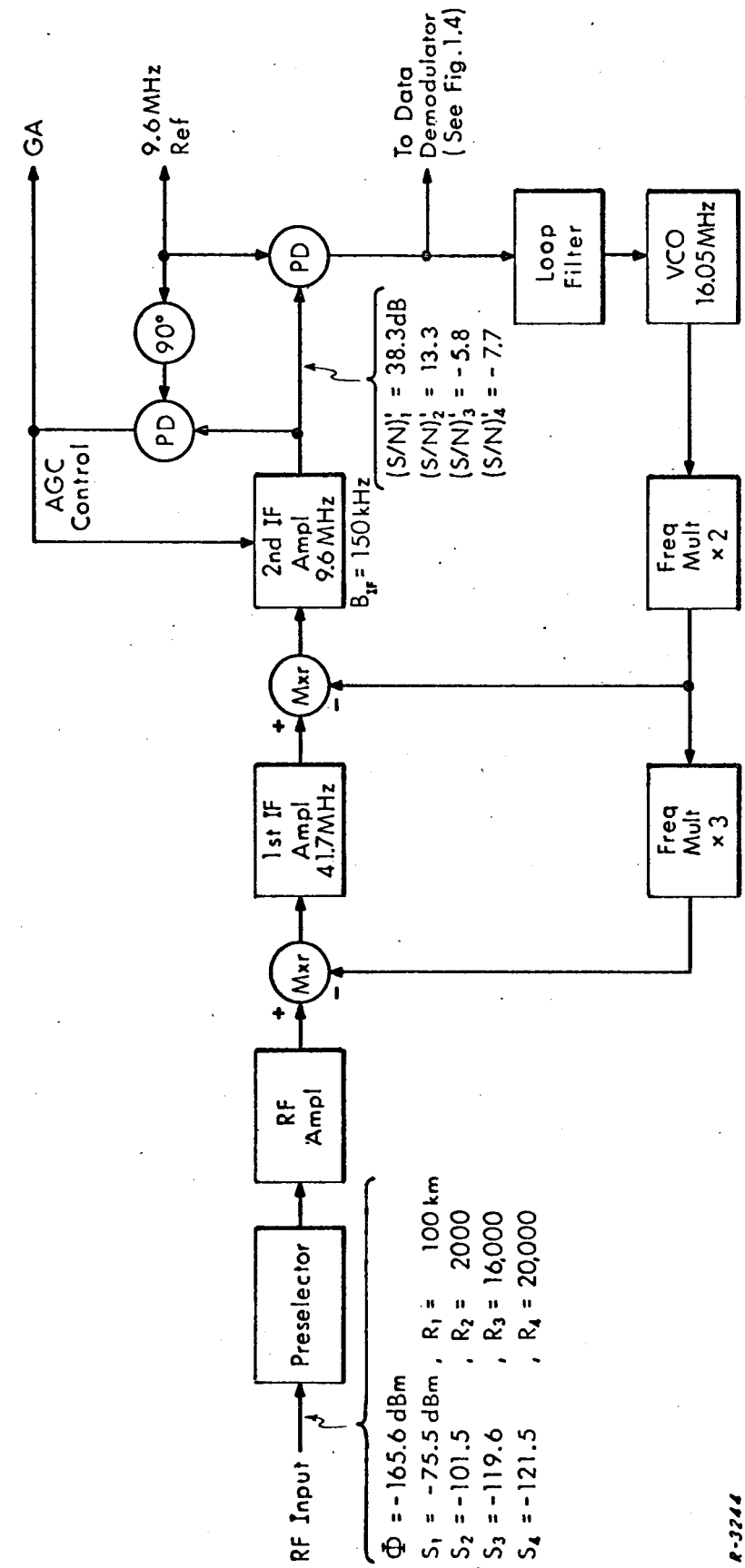

Fig. 2.3 Station Control Receiver (Part of Fig. 4-28, in Ref. 1)

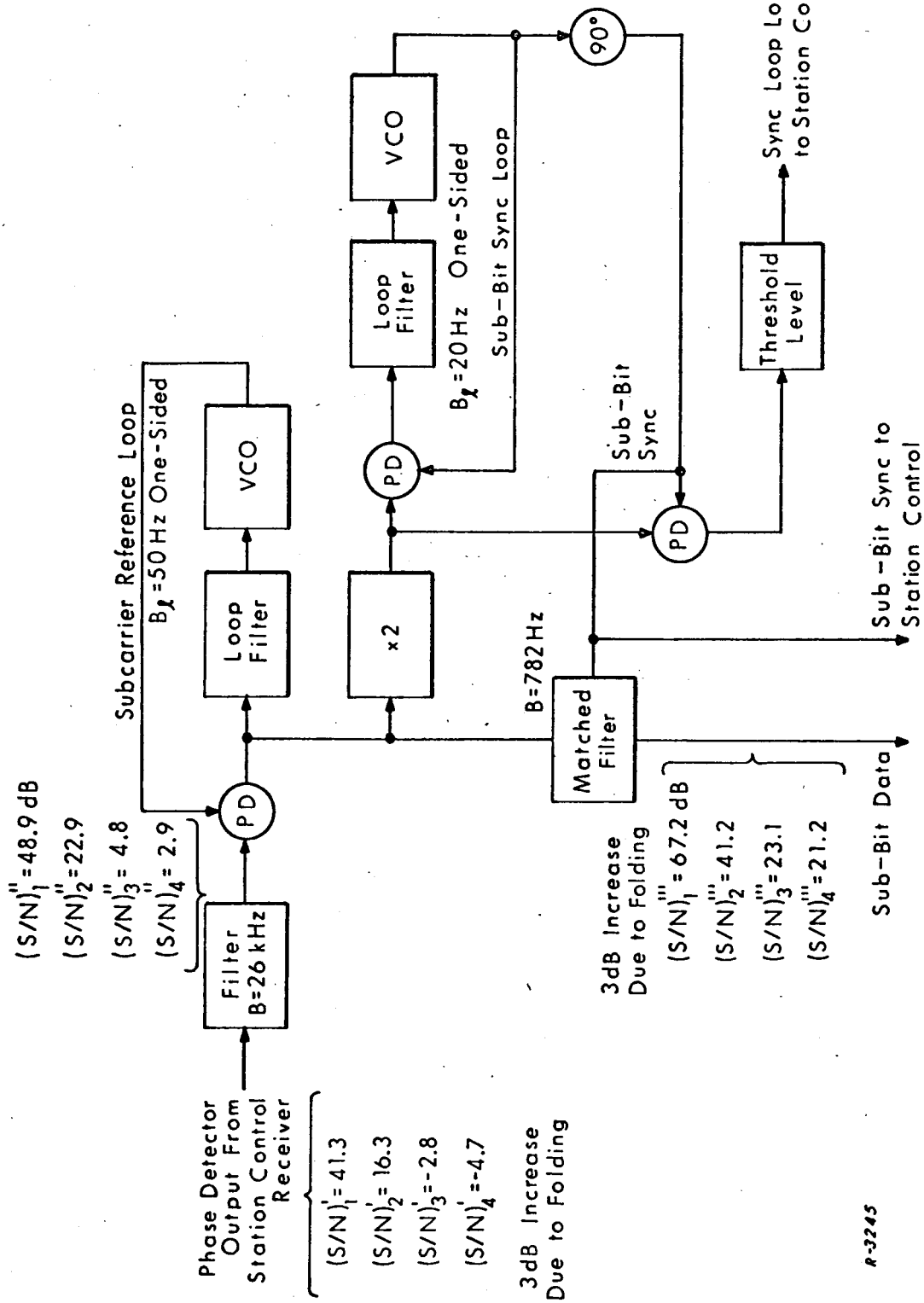

Fig. 2.4 Transponder Station Control Data Demodulator (Part of Fig. 4-28, in Ref. 1)

3. PERFORMANCE OF THE VTR CARRIER LOOP

3.1 Introduction

The carrier phase-locked loop (PLL) is the most important part of the VTR. Unless this loop properly tracks the carrier all uplink information is lost. Furthermore, the VTR carrier loop has several modes of operation resulting in a novel loop configuration. Thus much analysis has been done on the performance of this loop by ADCOM, and still more aspects appear to need further study.

There are three separate carrier loop analyses in this report. First, the model of the carrier loop is derived in the form of the conventional PLL. It is shown that carrier loop can be reduced to a standard second-order PLL with different dc and ac gains. This model is then employed in the following sections for the analysis of Dropout Memory Circuit which was being considered for the carrier loop. The memory circuit is an RC integrator. The design relationships for this circuit are presented, and it is shown that it only slightly affects the tracking performance of the carrier loop. Finally, in Sec. 3.3 the effects of transponder S-band antenna switching are analyzed. The S-band antenna is an array of 36 antenna elements. The array is switched by step phase changes at each antenna input. This results in amplitude and phase steps of the transmitted signal. The phase error in the VTR carrier loop due to these effects is obtained.

3.2 Derivation of the Loop Model*

The AROD system carrier loop is very difficult to represent with a phase transfer model. Since a linear phase transfer model is extremely useful

---

* This work was originally presented as ADCOM Technical Memorandum G-69-4, entitled, "Analysis of the Carrier Loop of the Vehicle Tracking Receiver in the AROD System," 14 October 1965.

for determining loop performance in terms of familiar loop parameters, it is worthwhile to develop some model of this form. Then, assuming the vehicle receiver is operating in state V-4 with no range tracking error, the carrier loop can be represented in an idealized way, as shown in Fig. 3.1.

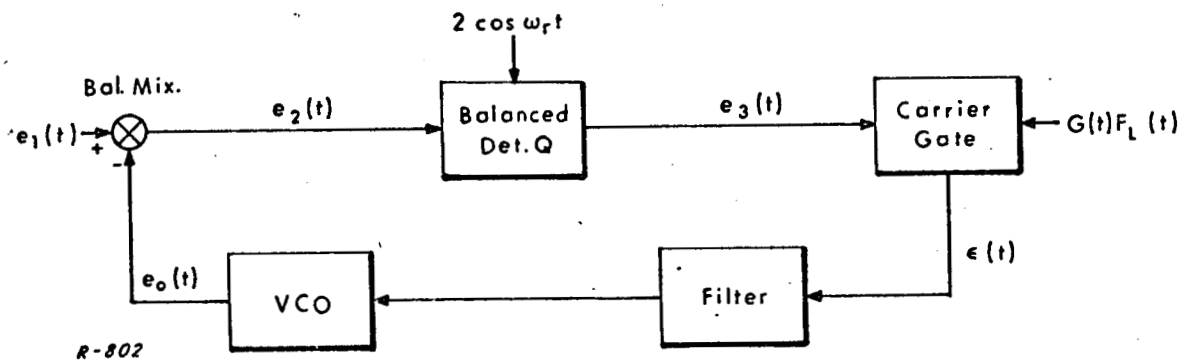

Fig. 3.1 Carrier Loop of the Vehicle Tracking Receiver.

The input $e_1(t)$ is

$$e_1(t) = F_L(t) \sin(\omega_1 t + \theta_1)$$

$$= \cos\left[\omega_1 t + \theta_1 - \frac{\pi}{2} F_L(t)\right] \qquad (3.1)$$

where $F_L(t)$ is a square wave of amplitude ± 1 and period T_L, equal to the L-code bit period

$$F_L(t) = \begin{cases} +1 & NT_L < t < \left(N + \frac{1}{2}\right) T_L \\ -1 & \left(N - \frac{1}{2}\right) T_L < t < NT_L \end{cases}$$

The carrier gate G(t) opens in the middle of each odd L-code bit so that $G(t)\,F_L(t)$ is as shown in Fig. 3.2.

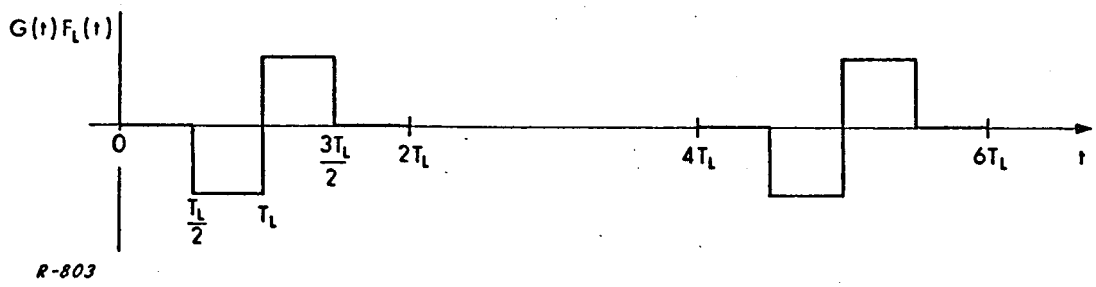

Fig. 3.2 The Function $G(t)\,F_L(t)$.

The signals at other points in the loop are:

$$e_o(t) = 2\cos\left[(\omega_1 - \omega_r)\,t + \theta_o\right] \tag{3.2}$$

$$e_2(t) = F_L(t)\sin(\omega_r t + \theta_1 - \theta_o)$$

$$= \cos\left[\omega_r t + \theta_1 - \theta_o - \frac{\pi}{2}F_L(t)\right] \tag{3.3}$$

$$e_3(t) = F_L(t)\sin(\theta_1 - \theta_o)$$

$$= \cos\left[\theta_1 - \theta_o - \frac{\pi}{2}F_L(t)\right] \tag{3.4}$$

$$\epsilon(t) = G(t)\sin(\theta_1 - \theta_o) \tag{3.5}$$

Equations (3.1) through (3.5) can be used to devise the phase transfer model of Fig. 3.3.

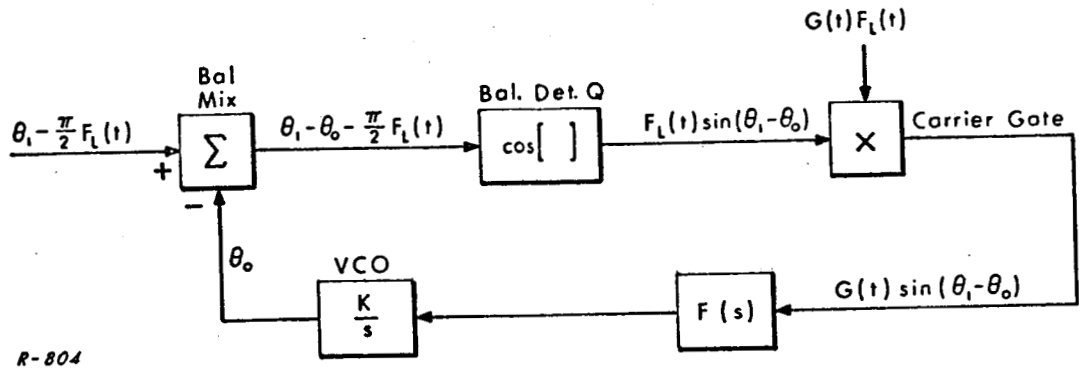

Fig. 3.3 Phase Transfer Model.

The model of Fig. 3.3 is not convenient because the gating functions appear and the variables are not consistent. Even if the range gating function did not appear in the model, it would still be difficult to use because it cannot be conveniently linearized. It is thus necessary to directly inspect the circuitry of the detector/gate/filter of the loop to derive a useful model.

The balanced detector Q consists of a transformer and two gates as included in Fig. 3.4 where the phase error $\theta_e = \theta_1 - \theta_o$.

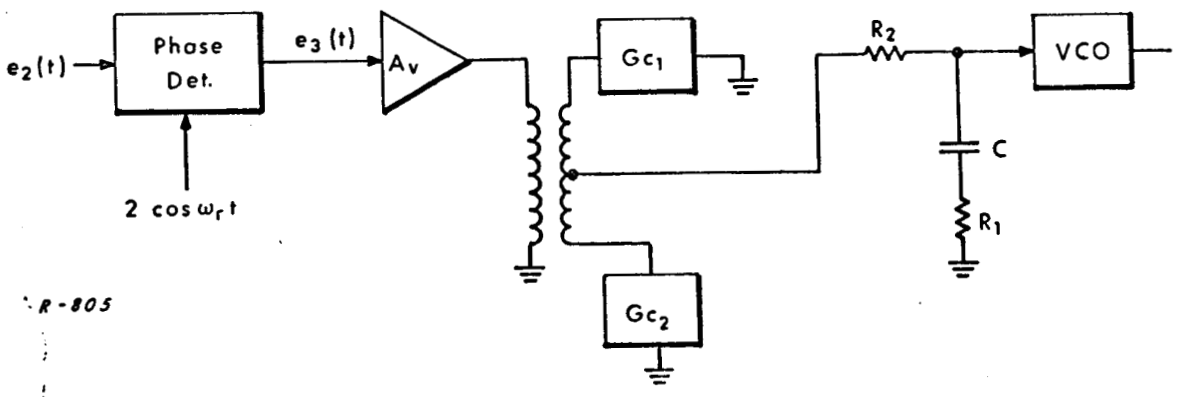

Fig. 3.4 Portion of Vehicle Tracking Receiver Carrier Loop.

The gates G_{c1} and G_{c2} are synchronized to the input in such a way that Fig. 3.4 can be redrawn as follows:

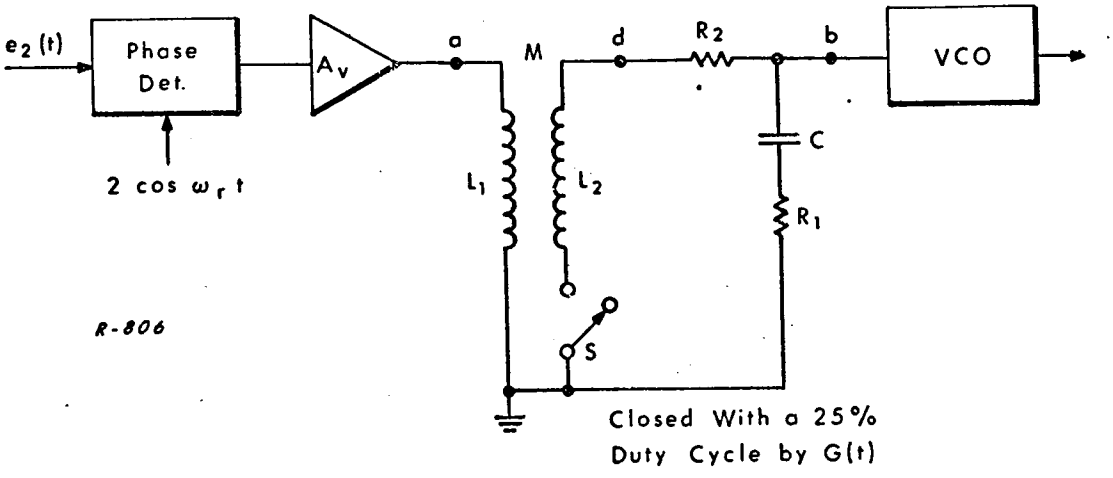

Fig. 3.5 An Equivalent Circuit of Fig. 3.4.

It is desirable to find a linear circuit to replace the circuit between point a and point b of Fig. 3.5. Unfortunately, because of the existence of the switch S an exact equivalent circuit cannot be found; furthermore, due to the fact that no dc component can pass through a transformer, the dc component appearing at the input of the lowpass filter is recovered partly by the switch S. Consequently, a further attenuation of the dc component results.

The dc component δ of the input can be handled as shown in Fig. 3.6. Thus δ can be calculated by the following equation:

$$(A_v E - \delta)\frac{T_L}{2} - \delta\frac{3T_L}{2} = 0 \qquad (3.6)$$

therefore

$$\delta = \frac{1}{4} A_v E \qquad (3.7)$$

Hence

$$A_v E - \delta = \frac{3}{4} A_v E \qquad (3.8)$$

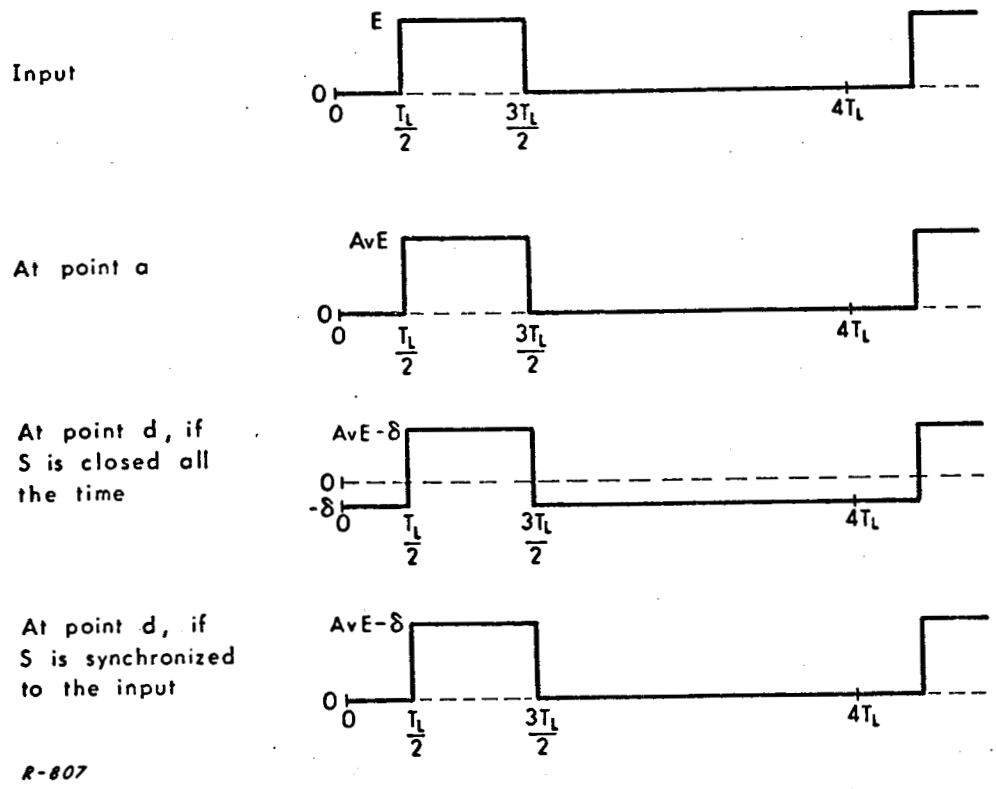

Fig. 3.6 Error Signal Waveforms.

The equivalent dc component appearing at the input of the VCO is then $\frac{3}{4} A_v E$, and the dc equivalent circuit of Fig. 3.4 is as shown in Fig. 3.7.

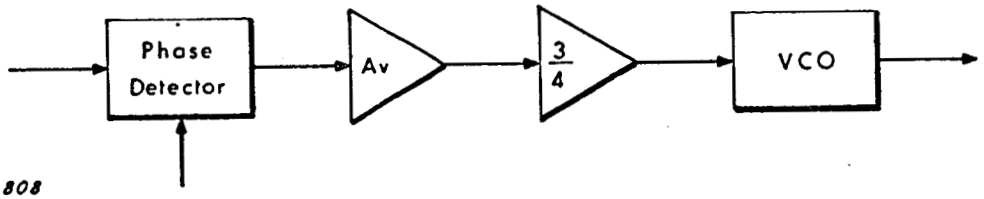

Fig. 3.7 DC Equivalent Circuit of Fig. 3.4.

Let us now find the equivalent circuit between a and b for the ac components. The switch is closed only 1/4 of the time, and during the period

when the switch is open there is no path for the capacitor to discharge if we assume the input impedance of the VCO is very high. This will effectively increase each time constant by a factor of 4. Therefore, the switch can be removed and the capacitor C replaced by 4C. The resultant equivalent circuit between a and b is drawn in Fig. 3.8.

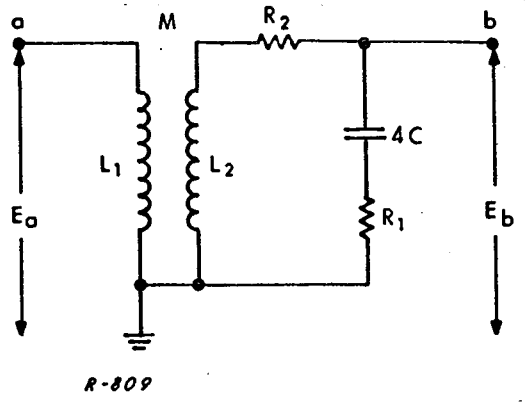

Fig. 3.8 AC Equivalent Circuit of Fig. 3.4.

The transfer function of Fig. 3.8 can be easily found to be

$$F(s) = \frac{E_b(s)}{E_a(s)} = \frac{\frac{M}{L_1}(s4R_1C + 1)}{s^2 4L_2C(1 - k^2) + s4(R_1 + R_2)C + 1} \qquad (3.9)$$

where, M is the mutual inductance of the transformer, L_1 and L_2 are the transformer primary and secondary leakage inductances respectively, and k is the coefficient of coupling.

Typically, L_2 is of the order of 10^{-3} henry, C about 10^{-6} farad, and $(1 - k^2)$ is not larger than 10^{-2}.

Hence

$$s^2 4 L_2 C (1 - k^2) \ll 1 \qquad (3.10)$$

and

$$s^2 4 L_2 C (1 - k^2) \ll s4 (R_1 + R_2) C \qquad (3.11)$$

for low frequencies. Therefore, the equivalent circuit can be represented in Fig. 3.9.

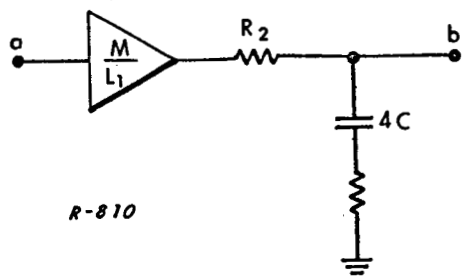

Fig. 3.9 Equivalent Circuit to Fig. 3.8.

And the complete equivalent linear circuit for Fig. 3.4 is given in Fig. 3.10.

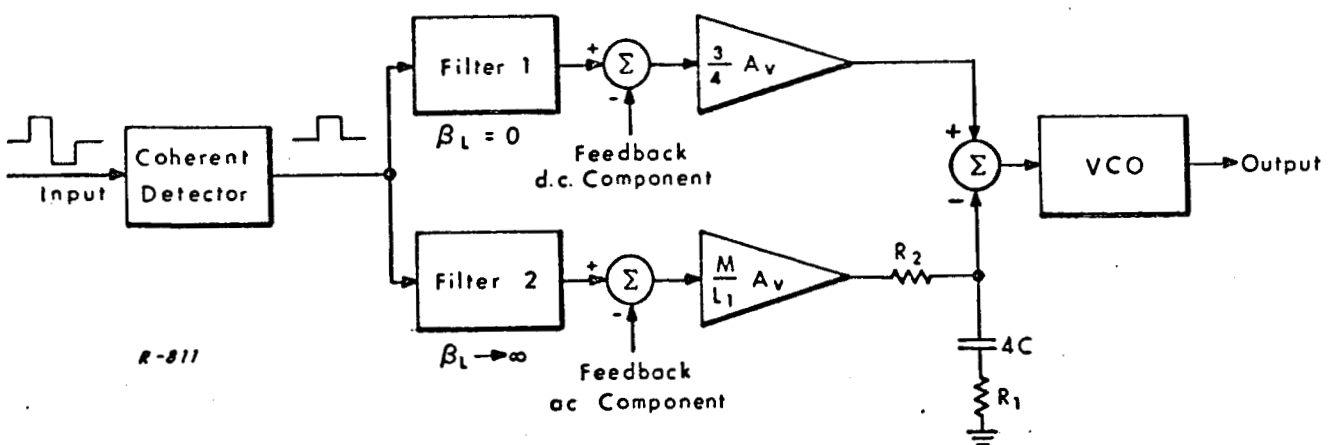

Fig. 3.10 Linear Equivalent Circuit of Fig. 3.4.

The Filter 1 is an idealized filter which can pass only the dc component while the Filter 2 can pass everything except the dc component.

It should be noted that the upper loop of Fig. 3.10 determines the center frequency of the output while the lower loop adds some noise to the output. The noise bandwidth and other parameters can be derived directly from the lower loop without referring to the upper loop.

From the lower loop of Fig. 3.10 the following equations can be obtained immediately:

$$K = \frac{M}{L_1} A_v \tag{3.12}$$

$$\tau_1 = 4R_1C \tag{3.13}$$

$$\tau_2 = 4(R_1 + R_2)C \tag{3.14}$$

$$\zeta = \sqrt{\frac{K}{4\tau_2}} \left[\tau_1 + \frac{1}{K}\right] = \frac{1}{4}\sqrt{\frac{MA_v}{(R_1+R_2)L_1C}} \left[4R_1C + \frac{L_1}{MA_v}\right] \tag{3.15}$$

$$B_n = \frac{\pi K}{\frac{1}{\tau_1} + K}\left[\frac{K\tau_1}{\tau_2} + \frac{1}{\tau_1}\right] = \frac{\pi \frac{M}{L_1} A_v}{\frac{1}{4R_1C} + \frac{MA_v}{L_1}}\left[\frac{M}{L_1} A_v \frac{R_1}{R_1+R_2} + \frac{1}{4R_1C}\right] \tag{3.16}$$

If we assume $M \approx L_1$, then

$$\zeta = \frac{1}{4}\sqrt{\frac{A_v}{(R_1+R_2)C}}\left[4R_1C + \frac{1}{A_v}\right]$$

$$= \sqrt{\frac{A_v}{(R_1+R_2)C}}\left[R_1C + \frac{1}{4A_v}\right] \tag{3.17}$$

$$B_n = \frac{\pi A_v}{\frac{1}{4R_1C} + A_v} \left[A_v \frac{R_1}{R_1 + R_2} + \frac{1}{4R_1C} \right] \tag{3.18}$$

Now, for comparison, consider a carrier loop without transformer and gates as shown in Fig. 3.11.

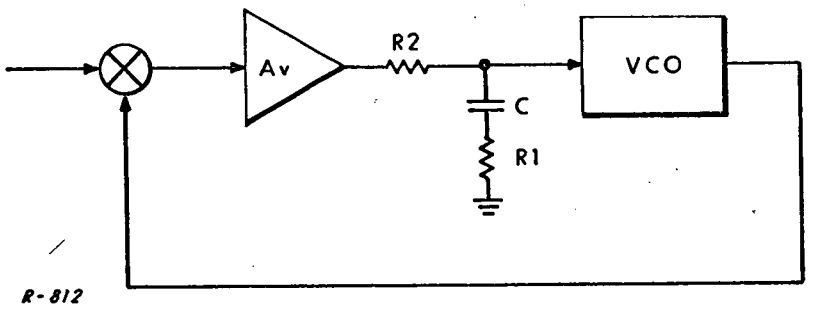

Fig. 3.11 Gated Input Loop for Comparison.

Since the input consists of pulses with a 25% duty cycle, we have

$$K' = \frac{1}{4} A_v \tag{3.19}$$

$$\tau_1' = R_1C \tag{3.20}$$

$$\tau_2' = (R_1 + R_2)C \tag{3.21}$$

$$\zeta' = \frac{1}{4} \sqrt{\frac{A_v}{(R_1 + R_2)C}} \left[R_1C + \frac{4}{A_v} \right] \tag{3.22}$$

$$B_n' = \frac{1}{4} \frac{\pi A_v}{\frac{4}{R_1C} + A_v} \left[\frac{A_v R_1}{R_1 + R_2} + \frac{1}{R_1C} \right] \tag{3.23}$$

If A_v is very large, we have

$$\zeta = 4\zeta' \tag{3.24}$$

$$B_n = 4B_n' \tag{3.25}$$

The balanced detector Q consisting of a transformer and two gates has two main effects on the loop as compared to a gated loop of a different configuration, (i) the dc gain is changed (in other words, the dc gain and the ac gain of the loop are different), and (ii) the damping ratio and the noise bandwidth of the loop are increased by a factor of 4. The noise bandwidth can be reduced, if necessary, by varying the amplification factor A_v, and the damping ratio can be adjusted to the desired value by choosing proper lowpass filter parameters. To match the dc and ac gains it is necessary to select the transformer so that the ratio $\frac{M}{L_1}$ equals the open loop attenuation of the dc component, which may not be a very practical choice. Thus we have shown that the carrier loop of the vehicle tracking receiver is a second-order phase-locked loop with different dc and ac gains. This model will be employed in the next section.

3.3 Analysis of Dropout Memory Circuit*

In this section we analyze the effect of a memory circuit being considered for dropout protection of the carrier loop. The memory is basically an RC integrator circuit in series with the loop filter and preceding it. If the input signal level drops rapidly the phase detector output is disconnected from these filters so that the RC integrator retains its previous charge and the VCO

* This work was originally presented in ADCOM Technical Memorandum G-69-5, entitled, "The Effect of Memory Circuit on the Carrier Loop Performance in the VTR in the AROD System," 19 November 1965.

its previous frequency. Thus if the signal dropout is for a short interval there is little loss of time to acquire again.

As shown in the section above, the carrier loop of the vehicle tracking receiver is a second-order phase-lock loop with different dc and ac gains. For the sake of simplicity, in this section the dc component and the ac components of the carrier loop are not analyzed separately; all the results can be applied to both the dc and ac components of the carrier loop by properly interpreting K as the dc or ac loop gain.

An extra integrator is inserted in the carrier loop to serve as a memory circuit during input signal dropout periods as shown in Fig. 3.12.

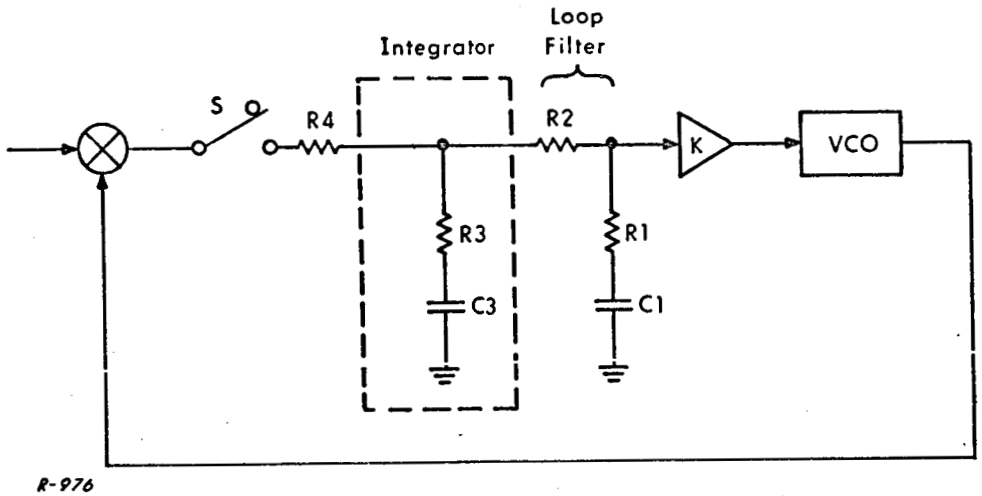

Fig. 3.12 Carrier Loop with Dropout Protection Circuitry.

The switch S is closed except for a brief interval when the input signal disappears or is too weak for the loop to track. R_2 is assumed much larger than R_3 so that the loop filter will not load severely on the R-C stage consisting of R_4 and the integrator. In order to provide proper "memory" during the input signal dropout periods, the time constant $\tau_4 = (R_3 + R_4) C_3$ should be much smaller than $\tau_2 = (R_1 + R_2) C_1$; and $C_3 >> C_1$ so that a small portion of the charge stored in C_3, when S is open, is sufficient to charge up

C_1 to its steady state voltage. With all these assumptions, we can then proceed to investigate the effect on the carrier loop due to the insertion of the integrator.

The transfer function of the integrator together with the loop filter is approximately given by

$$F(s) = \frac{1+\tau_3 s}{1+\tau_4 s} \cdot \frac{1+\tau_1 s}{1+\tau_2 s}, \tag{3.26}$$

where,

$$\tau_1 = R_1 C_1, \tag{3.27}$$

$$\tau_2 = (R_1+R_2)C_1, \tag{3.28}$$

$$\tau_3 = R_3 C_3, \tag{3.29}$$

$$\tau_4 = (R_3+R_4) C_3 \tag{3.30}$$

The loop transfer function is then

$$H(s) = \frac{KF(s)}{s+KF(s)}$$

$$= \frac{K\left[1+(\tau_1+\tau_3)s+\tau_1\tau_3 s^2\right]}{K+\left[K(\tau_1+\tau_3)+1\right]s+(K\tau_1\tau_3+\tau_2+\tau_4)s^2+\tau_2\tau_4 s^3} \tag{3.31}$$

The two-sided noise bandwidth B_n can be calculated by the following formula:

$$B_n = \frac{1}{2\pi}\int_{-\infty}^{\infty} |H(j\omega)|^2 \, d\omega \text{ Hz} \tag{3.32}$$

Substituting Eqn. (3.31) in (3.32) we obtain:

$$B_n = \frac{K\left\{K\tau_1^2\tau_3^2\left[K(\tau_1+\tau_3)+1\right]+K(\tau_1^2+\tau_3^2)\tau_2\tau_4+(K\tau_1\tau_3+\tau_2+\tau_4)\tau_2\tau_4\right\}}{2\tau_2\tau_4\left\{-K\tau_2\tau_4+\left[K(\tau_1+\tau_3)+1\right](K\tau_1\tau_3+\tau_2+\tau_4)\right\}} \tag{3.33}$$

By looking at Eq. (3.33), it is difficult to find a general relation among B_n, τ_3 and τ_4 for fixed values of τ_1, τ_2 and K. Therefore, we must find a way to simplify Eq. (3.33).

The parameters of the carrier loop are given approximately as the following:

$$K \approx 9 \times 10^{6} \text{ sec}^{-1}$$
$$\tau_1 \approx 3.75 \times 10^{-3} \text{ sec}$$
$$\tau_2 \approx 60 \text{ sec}$$

Let us assume that the values of τ_3 and τ_4 are less than 6 sec ($\approx \frac{1}{10}\tau_2$). Then we have:

$$K(\tau_1 + \tau_3) \gg 1$$

therefore

$$B_n \approx \frac{K\left\{K^2\tau_1^2\tau_3^2(\tau_1+\tau_3) + K\tau_3^2\tau_2\tau_4 + (K\tau_1\tau_3+\tau_2+\tau_4)\tau_2\tau_4\right\}}{2\tau_2\tau_4\left\{-K\tau_2\tau_4 + K(\tau_1+\tau_3)(K\tau_1\tau_3+\tau_2+\tau_4)\right\}}$$

$$= \frac{K^2\tau_1^2\tau_3^2(\tau_1+\tau_3) + [K(\tau_1+\tau_3)\tau_3+\tau_2+\tau_4]\tau_2\tau_4}{2\tau_2\tau_4\left\{-\tau_2\tau_4 + (\tau_1+\tau_3)(K\tau_1\tau_3+\tau_2+\tau_4)\right\}} \qquad (3.34)$$

Now,

$$K(\tau_1+\tau_3)\tau_3 \geq 9 \times 10^{6} \times (3.75 \times 10^{-3} + 2 \times 10^{-1}) \times 2 \times 10^{-1}$$
$$> 36 \times 10^{4}$$

and

$$\tau_2 + \tau_4 \approx 60 + 6 = 66$$

$$\therefore K(\tau_1+\tau_3)\tau_3 \gg \tau_2 + \tau_4$$

Equation (3.34) can then be rewritten as

$$B_n \approx \frac{K^2 \tau_1^2 \tau_3^2 (\tau_1 + \tau_3) + K(\tau_1 + \tau_3)\tau_3 \tau_2 \tau_4}{2\tau_2\tau_4\left[-\tau_2\tau_4 + (\tau_1+\tau_3)(K\tau_1\tau_3 + \tau_2 + \tau_4)\right]}$$

$$= \frac{K\tau_3(\tau_1+\tau_3)(K\tau_1^2\tau_3 + \tau_2\tau_4)}{2\tau_2\tau_4\left[K(\tau_1+\tau_3)\tau_1\tau_3 + \tau_2\tau_1 + \tau_2\tau_3 - \tau_2\tau_4 + \tau_4\tau_1 + \tau_3\tau_4\right]} \qquad (3.35)$$

But,

$$K(\tau_1 + \tau_3)\tau_1\tau_3 > 1350 \qquad (3.36)$$

$$\tau_2\tau_1 + \tau_2\tau_3 - \tau_2\tau_4 + \tau_4\tau_1 + \tau_3\tau_4$$

$$= \tau_2\tau_1 + \tau_2\tau_3 - (\tau_2 - \tau_1)\tau_4 + \tau_3\tau_4$$

$$\approx \tau_2\tau_1 + \tau_2\tau_3 - \tau_2\tau_4 + \tau_3\tau_4 \qquad \text{since } \tau_1 \ll \tau_2$$

$$\approx \tau_2\tau_1 + \tau_2\tau_3 - \tau_2\tau_4 + \frac{1}{10}\tau_3\tau_2, \qquad \text{since } \frac{\tau_2}{10} \gtrsim \tau_4$$

$$- \tau_2\tau_1 + \frac{11}{10}\tau_2\tau_3 - \tau_2\tau_4$$

$$= \tau_2\tau_1 + \tau_2\left(\frac{11}{10}\tau_3 - \tau_4\right)$$

$$= 60 \times 3.75 \times 10^{-3} + \tau_2\left(\frac{11}{10}\tau_3 - \tau_4\right)$$

$$= 0.225 + 60\left(\frac{11}{10}\tau_3 - \tau_4\right) \qquad (3.37)$$

In order to make $60\left(\frac{11}{10}\tau_3 - \tau_4\right) \ll 1350$ and $\tau_3 < \tau_4$ we require that

$$\frac{11}{10}\tau_3 - \tau_4 \leq \frac{1}{10}, \text{ or } \frac{11}{10}\tau_3 \leq \tau_4 + \frac{1}{10} \qquad (3.38)$$

For maximum value of τ_4, i.e., for $\tau_4 = 6$:

$$\frac{11}{10}\tau_3 \leq \frac{61}{10}$$

$$\tau_3 \leq \frac{61}{11} \tag{3.39}$$

which implies that as long as

$$\frac{\tau_3}{\tau_4} < \frac{\frac{61}{11}}{6} = \frac{61}{66} = 0.925 \text{ and } \tau_4 \leq 6,$$

the following condition will be satisfied:

$$K(\tau_1+\tau_3)\tau_1\tau_3 >> \tau_2\tau_1 + \tau_2\tau_3 - \tau_2\tau_4 + \tau_4\tau_1 + \tau_3\tau_4$$

Then Eq. (3.35) becomes

$$B_n \approx \frac{K\tau_3(\tau_1+\tau_3)(K\tau_1^2\tau_3 + \tau_2\tau_4)}{2\tau_2\tau_4 K(\tau_1+\tau_3)\tau_1\tau_3}$$

$$= \frac{K\tau_1^2\tau_3 + \tau_2\tau_4}{2\tau_1\tau_2\tau_4}$$

$$= \frac{1}{2}\left[K\left(\frac{\tau_1}{\tau_2}\right)\left(\frac{\tau_3}{\tau_4}\right) + \frac{1}{\tau_1}\right], \tag{3.40}$$

provided

$$\tau_4 < 6 \text{ sec}, \tag{3.41}$$

and

$$\frac{\tau_3}{\tau_4} < 0.925 \tag{3.42}$$

The noise bandwidth of a standard second-order loop with high open loop gain K' can be expressed as

$$B_n' = \frac{1}{2}\left[K'\left(\frac{\tau_1'}{\tau_2'}\right) + \frac{1}{\tau_1'}\right] \tag{3.43}$$

By comparing Eqs.(3.40) and (3.43), we know that the noise bandwidth is decreased due to the insertion of the integrator since $\tau_3/\tau_4 < 1$ and it is a linear function of (τ_3/τ_4). In order to minimize the effect of the integrator on the noise bandwidth, we have to make the ratio R_4/R_3 as small as possible. But R_4 is the resistance associated with the phase detector. Its value cannot be varied and the only thing we can do is to make R_3 as large as possible. By doing this, the time constants τ_3 and τ_4 may become too large since C_3 is a large capacitor. Therefore, a reasonable value of R_3 should be chosen so that it will not make τ_3 and τ_4 too large, and meanwhile will not reduce the noise bandwidth of the loop drastically.

The easiest way to see the effect on the damping ratio due to the insertion of the integrator is to investigate the change of root loci of the loop by introducing a zero at $s = -1/\tau_3$ and a pole at $s = -1/\tau_4$. Figure 3.13 is the root locus plot of a standard second-order loop with a filter transfer function $\left(1+\tau_1\right)/\left(1+\tau_2\right)$, and the damping ratio for K_1 is cos θ' as shown in the figure. When an integrator is inserted the root locus plot is shown in Fig. 3.14.

Because the extra zero and pole appear at $s = -\frac{1}{\tau_3}$ and $s = -\frac{1}{\tau_4}$ respectively, for the same value of K_1, we will have $\theta' < \theta$ or $\zeta' > \zeta$. The damping ratio of the carrier loop is also decreased due to the insertion of the integrator. To find the exact relation among ζ, τ_3, and τ_4 will be difficult

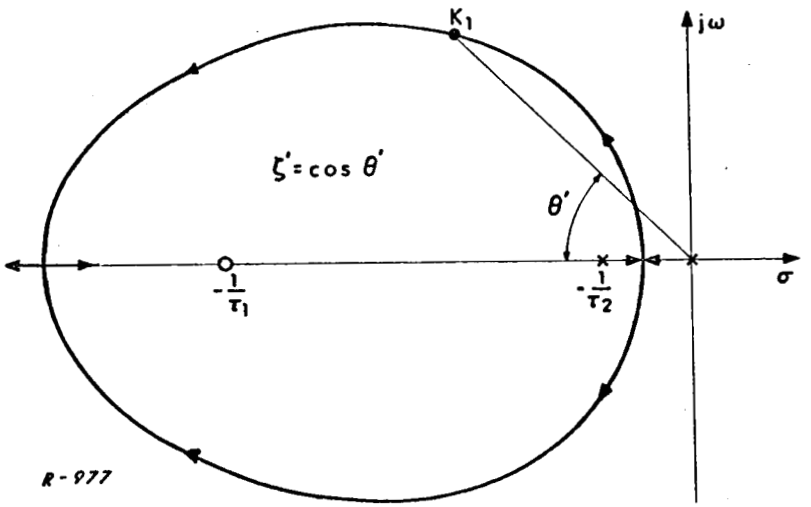

Fig. 3.13 Root Locus Plot of a Standard Second-Order Loop Containing the Filter $F(s) = (1+\tau_1 s)/(1+\tau_2 s)$.

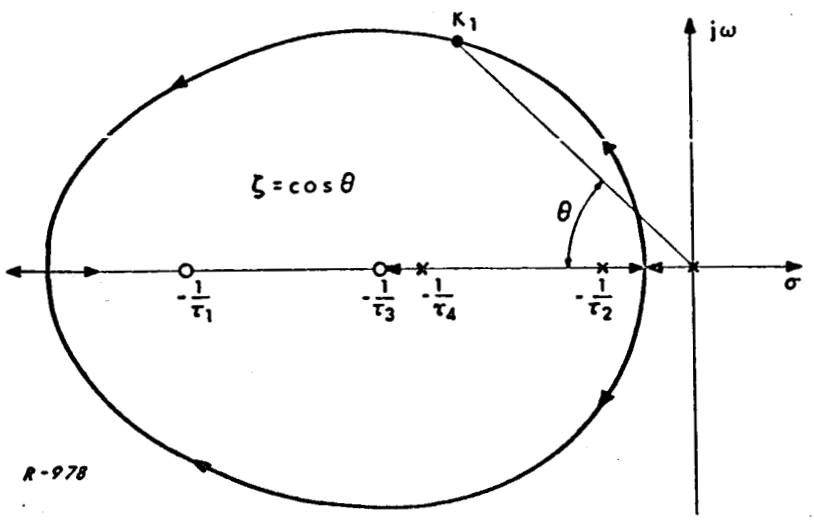

Fig. 3.14 Root Locus Plot for the Carrier Loop with $F(s) = (1+\tau_3 s)/(1+\tau_4 s) \cdot (1+\tau_1 s)/(1+\tau_2 s)$.

because it involves solving the roots for the denominator of the loop transfer function (Eq. (3.31), i.e.,

$$K + \left[K\left(\tau_1 + \tau_3\right) + 1\right] s + \left[K\tau_1\tau_3 + \tau_3 + \tau_4\right] s^2 + \tau_2\tau_4 s^3 = 0$$

An intuitive way of relating ζ, τ_3 and τ_4 is then necessary in order to have a better insight into the carrier loop. Let us investigate once more Eq. (3.40) which can be rewritten as

$$B_n = \frac{1}{2}\left[\left(\frac{\tau_3}{\tau_4} K\right)\left(\frac{\tau_1}{\tau_2}\right) + \frac{1}{\tau_1}\right] \tag{3.44}$$

It looks like the insertion of the integrator does nothing to the loop except to modify its open loop gain; in other words, the integrator together with R_4 can be considered as a voltage divider which attenuates the open loop gain by a factor of $\tau_3/\tau_4 < 0.925$. Then we can assume that the damping ratio is a linear function of $\sqrt{\frac{\tau_3}{\tau_4}}$, because ζ is a linear function of $\sqrt{K}$.

The carrier loop input and the voltage fed into the filter are gated synchronously with a 25% duty cycle as mentioned in Sec. 3.1. Because of the gating, the time constants of the integrator and the filter may need some modification. Considering Fig. 3.15, since $R_2 \gg R_3$, e_2 is nearly unchanged

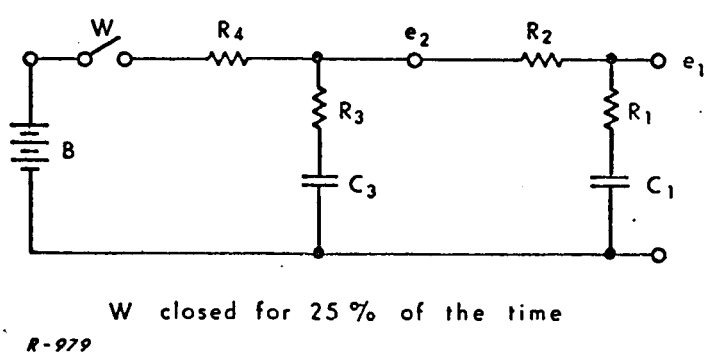

Fig. 3.15 Circuit for Finding Equivalent Time Constants.

whether the loop filter is connected to the integrator or not. It is evident that the time constant of the integrator is increased by a factor of 4 if we assume that the input is gated. The voltage appearing at e_2 charges C_1 continuously whether the switch W is closed or not, which will not reduce the voltage e_2 significantly even when W is open because $C_3 >> C_1$. At 5 time constants, i.e., $5\left[4\left(R_3 + R_4\right) C_3\right]$ sec, e_2 reaches its steady state value. But $\left[20\left(R_3 + R_4\right) C_3\right]$ is just a small fraction of $5\left(R_1 + R_2\right)C_1$ and, furthermore, at $\left[20\left(R_3 + R_4\right) C_3\right]$ sec, e_1 has been charged to a certain value already. Hence, we can safely conclude that the time constants of the filter are unaltered due to the gating of the carrier loop. By the above argument, the Eqs. (3.29) and (3.30) should be modified as

$$\tau_3 = 4R_3C_3 \tag{3.29a}$$

$$\tau_4 = 4(R_3+R_4)C_3 \tag{3.30a}$$

We now proceed to compare the dynamic error of a standard second-order PLL and that of the carrier loop under investigation.

For a standard second-order PLL with $\left(1+\tau_1 s\right)/\left(1+\tau_2 s\right)$ as the filter transfer function, its error transfer function can be expanded as an infinite series:

$$E'(s) = \frac{1}{K}s + \frac{\tau_2}{K}s^2 - \frac{\tau_1\tau_2}{K}s^3 + \ldots \tag{3.45}$$

If the input is $\psi(t)$, then the dynamic error for the second-order PLL is

$$\theta'_{ed}(t) = \frac{1}{K}\frac{d}{dt}\psi(t) + \frac{\tau_2}{K}\frac{d^2}{dt^2}\psi(t) - \frac{\tau_1\tau_2}{K}\frac{d^3}{dt^3}4(t) + \ldots \tag{3.46}$$

When an integrator is inserted:

$$E(s) = 1 - H(s) \tag{3.47}$$

Substituting Eq. (3.31) in Eq. (3.33), we have

$$E(s) = \frac{s + (\tau_2 + \tau_4)\, s^2 + \tau_2 \tau_4 s^3}{K + \left[K(\tau_1 + \tau_3) + 1\right] s + (K\tau_1\tau_3 + \tau_2 + \tau_4) s^2 + \tau_2 \tau_4 s^3}$$

$$\approx \frac{s + (\tau_2 + \tau_4) s^2 + \tau_2 \tau_4 s^3}{K + K(\tau_1 + \tau_3)\, s + (K\tau_1\tau_3 + \tau_2)\, s^2 + \tau_2 \tau_4 s^3} \qquad (3.48)$$

By long division, we obtain

$$E(s) \approx \frac{1}{K} + \frac{\tau_2}{K} s^2 - \left[\frac{\tau_1\tau_2}{K} - \frac{\tau_2(\tau_4 - \tau_3)}{K}\right] s^3 + \ldots \qquad (3.49)$$

$$\theta_{ed}(t) = \frac{1}{K}\frac{d}{dt}\psi(t) + \frac{\tau_2}{K}\frac{d^2}{dt^2}\psi(t) - \left[\frac{\tau_1\tau_2}{K} - \frac{\tau_2(\tau_4 - \tau_3)}{K}\right]\frac{d^3}{dt^3}\psi(t) + \ldots \qquad (3.50)$$

It can be easily seen that when

$$\frac{d^n}{dt^n}\psi(t) = o \quad \text{for } n \geq 3, \qquad (3.51)$$

which implies that

$$\psi(t) = b_o + b_1 t + b_2 t^2 \qquad (3.52)$$

then

$$\theta'_{ed}(t) = \theta_{ed}(t)$$

In other words, the insertion of an integrator into a second-order PLL will not affect its dynamic error if the phase input contains only phase steps, frequency steps and frequency ramps.

From the above analysis, we can conclude that the carrier loop of the vehicle tracking receiver of the AROD system can be treated as a slightly modified second-order loop when it operates properly, the integrator of the loop will reduce the loop noise bandwidth and damping ratio very slightly and will not affect the dynamic error which appears in the AROD system by the proper choice of the integrator parameters. When the input signal is too weak or disappears completely, the integrator is disconnected from the output of the phase detector and it then serves as a memory element.

3.4 Effects of Transponder S-Band Antenna Switching*

The electronically steered S-band antenna array of an AROD transponder consists of 36 antenna elements arranged in a 6 x 6 square matrix. The beam of the array which points in the desired direction is chosen by step phase changes to the input of each antenna element so that the radiation pattern of the total array is directed toward the vehicle. When the radiation pattern changes, there are also changes in the phase and amplitude of the signal. A maximum of ± 3 dB variation in amplitude has been indicated and various phase values between 10^{o} and 1 radian have been mentioned. In the following analysis, the additional phase error in the carrier loop due to the step changes in input signal level and phase will be estimated.

Victor and Brockman[4] have developed a linearized AGC loop model for coherent AGC systems, with a transfer function relating input amplitude changes (in dB) to amplifier attenuation changes (also in dB) which is

$$H_a(s) = \frac{1}{\left(\frac{1}{G} + 1\right) + \frac{\tau}{G} s} \tag{3.53}$$

where G is the AGC loop gain and τ is the loop filter time constant.

---

* This work was originally presented in ADCOM Technical Memorandum G-69-9, entitled, "Effect of S-Band Antenna Switching Phase and Amplitude Step Changes on Carrier Loop of VTR," 20 May 1966.

The corresponding impulse response h(t) is

$$h(t) = \frac{G}{\tau} e^{-\frac{G+1}{\tau}t} \tag{3.54}$$

The impulse response can be integrated to get the step response f(t)

$$f(t) = \int_0^t h(t)\, dt = \frac{1}{1+\frac{1}{G}} \left(1 - e^{-\frac{G+1}{\tau}t}\right) \tag{3.55}$$

The vehicle receiver AGC has $\tau = 0.35$ sec and G which varies from $G_S = 260$ at strong signals to $G_T = 19.2$ at the threshold of the AGC. If the input level to the receiver undergoes a 3 dB step change represented by $\Delta a = \pm 3$ dB at $t = 0$ the additional IF amplifier attenuation $a^*(t)$ (in dB) resulting from this input will be

$$a^*(t) = \pm 3\, f(t)\ \text{dB} \approx \pm 3 \left(1 - e^{-\frac{G+1}{\tau}t}\right)\ \text{dB} \qquad t \geq 0 \tag{3.56}$$

The output variation of the IF amplifier is

$$\Delta a - a^*(t) = \pm 3\, e^{-\frac{G+1}{\tau}t}\ \text{dB} \qquad t \geq 0 \tag{3.57}$$

or, converting from a logarithmic to a linear description we let $a = 20 \log_{10} A$,

$$A_o(t) = \frac{\Delta A}{A^*}(t) = 10^{\pm 0.15}\, e^{-\frac{G+1}{\tau}t} \qquad t \geq 0 \tag{3.58}$$

This response is shown in Fig. 3.16. At $t = 0$

$$A_o(0) = \begin{cases} 1.413 \\ 0.708 \end{cases} \text{ or} \tag{3.59}$$

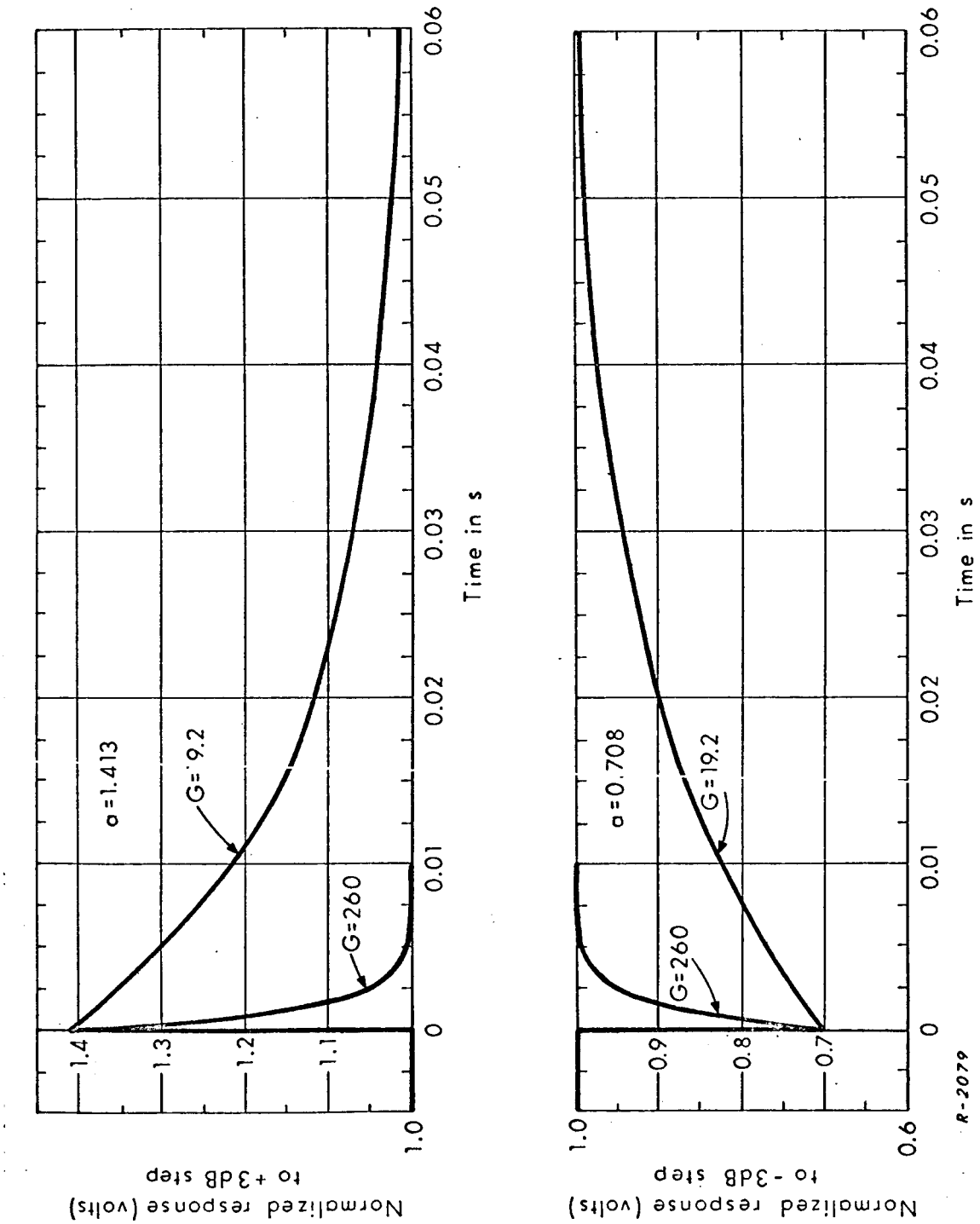

Fig. 3.16 IF Amplifier Output Level with Input Level Step.

Then for this range of amplitude steps the gain constant of the carrier loop can vary between the limits 0.708 K and 1.413 K, where K is the normal value, the variation due to the fluctuation of the input amplitude level.

The exact effect of an input amplitude variation of the form

$$E_{in}(t) = \begin{cases} 1 & t < 0 \\ 10^{\pm 0.15\, e^{-\frac{G+1}{0.35} t}} & t \geq 0 \end{cases} \qquad (3.60)$$

on the carrier loop is difficult to determine. For $t>0$ the system gain is time varying. It is possible to write an equation which contains the loop phase error as a function of time but the equation cannot readily be solved. A linear approximation to the gain variation is not useful as the equation still cannot be solved. The only approach yielding an answer is to let the gain undergo a step change to either 0.708 K or 1.413 K. This approach will produce an upper bound to the phase error. This assumption is identical to assuming that the AGC system is inoperative or has an infinite time constant, so that the approximate answer will be more correct the wider the carrier loop bandwidth and the slower the AGC loop response time. This point will be discussed in more detail later.

If the carrier loop gain variation has the form of a step, the system transfer function can be used in the evaluation. Let us assume the carrier loop is originally locked to an input signal having doppler shift Ωrad/sec and that a steady-state phase error condition has been reached. Then simultaneous step changes in both input phase and level occur. The change in level will alter the loop gain, thus changing the closed loop transfer function and creating a time-varying system having two fixed states. In the system's first state the loop phase error is constant at

$$E_o = \frac{\Omega}{K} \text{ radians} \qquad (3.61)$$

In the second state both step changes will cause additional phase errors to appear. The phase step occurs as the system changes parameter values, so the error is then simply the error of the second system to the phase step, provided nothing makes the linear loop model invalid in either state.

The amplitude step will affect the loop error to doppler and can be analyzed by considering an equivalent phase step input to the second system. The value of equivalent phase step can be found in the following way. The phase detector output is initially

$$E_{p_o} = \frac{\Omega}{K} \cdot K_d \text{ volts} \tag{3.62}$$

where K_d is the phase detector gain in v/rad. Immediately after the system changes states (i.e., the steps occur) the phase detector output will be

$$E_{p_2} = \frac{\Omega}{K} \cdot aK_d \text{ volts} \tag{3.63}$$

because the phase detector gain must change with the input level change. There cannot be any change in loop phase error (Ω/K) at this point. We now have the loop in its second state with the "initial condition" of E_{p_2}. This condition is indistinguishable from that where we introduce a suitable phase step into the loop. In both cases the only immediate effect is a change in phase detector output.

We can write the phase detector output just after the change to the system second state as the sum of doppler error and equivalent step phase error Ψ radians

$$E_{p_2} = \frac{\Omega}{aK} \cdot aK_d + \Psi a K_d \tag{3.64}$$

Equating Eqs. (3.63) and (3.64) and solving for Ψ gives

$$\Psi = \frac{a-1}{a} \cdot \frac{\Omega}{K} \tag{3.65}$$

which is a function of Ω as would be expected.

The phase error (transform) to a phase step input is

$$E_s(s) = [1 - H_2(s)] \frac{\Psi + \Phi}{s} \tag{3.66}$$

where the actual phase step input Φ is also included, and where $H_2(s)$ is the loop transfer function in the second state. Then

$$E_s(s) = \frac{\tau_2 s + 1}{\tau_2 s^2 + (aK\tau_1 + 1)s + aK} \cdot \frac{\frac{(a-1)\Omega}{aK} + \Phi}{s} \tag{3.67}$$

The system response to the step is the inverse transform

$$e_s(t) = \left[\frac{(a-1)\Omega}{aK} + \Phi\right] (\operatorname{cosec}\phi) e^{-\frac{aK\tau_1+1}{2\tau_2}t} \sin\left[\sqrt{\frac{aK}{\tau_2} - \left(\frac{aK\tau_1+1}{2\tau_2}\right)^2}\, t - \phi + \pi\right] \tag{3.68}$$

where

$$\phi = \tan^{-1} \sqrt{\frac{4aK(\tau_2 - \tau_1)}{(K\tau_1 - 1)^2} - 1} \tag{3.69}$$

The total loop phase error before the steps occur (before $t = 0$) was found to be Ω/K radians. After the change the error will be the sum of the step response $e_s(t)$ and a constant $\Omega/(aK)$ which represents the error initially in the loop. Then

$$e(t) = \begin{cases} \frac{\Omega}{K} \text{ rad} & t \le 0 \qquad (3.70a) \\ \frac{\Omega}{aK} + e_s(t) \text{ rad} & t \ge 0 \qquad (3.70b) \end{cases}$$

We may determine a worst case of inputs which will produce the largest magnitude of e(t). The most unfavorable condition occurs when a = 0.708. In addition the peak error varies with the magnitudes of the initial doppler error and the phase step. We shall assume that the phase step has value $\Phi = -10^{\circ}$. The carrier loop parameters are

$$K = 2.25 \times 10^{6} \text{ sec}^{-1}$$
$$\tau_1 = 3.75 \times 10^{-3} \text{ sec}$$
$$\tau_2 = 15.75 \text{ sec}$$

The maximum expected doppler shift is 72 kHz, so the maximum initial doppler error is

$$\frac{\Omega}{K} = \frac{2\pi \times 7.2 \times 10^{4}}{2.25 \times 10^{6}} = 0.201 \text{ rad}$$

Under these conditions

$$e(t) = \begin{cases} 0.201 \text{ rad} & t < 0 \\ 0.284 - 0.479\, e^{-189\,t} \sin[255\,t + 2.57] \text{ rad} & t \ge 0 \end{cases} \qquad (3.71)$$

which is plotted in Fig. 3.17a. The peak phase error is seen to be about 0.41 radian (23.5°) and should not cause any serious problems. The peak occurs approximately 6 ms after the steps, at which time Fig. 3.16 shows that the AGC has been able to correct 30% (in voltage) of the amplitude step, assuming the minimum AGC loop gain. Therefore the approximation of the loop gain variation as a step change provides an adequate bound, but Eq. (3.70) does not accurately represent the actual phase error in the loop and the curve of Fig. 3.17a

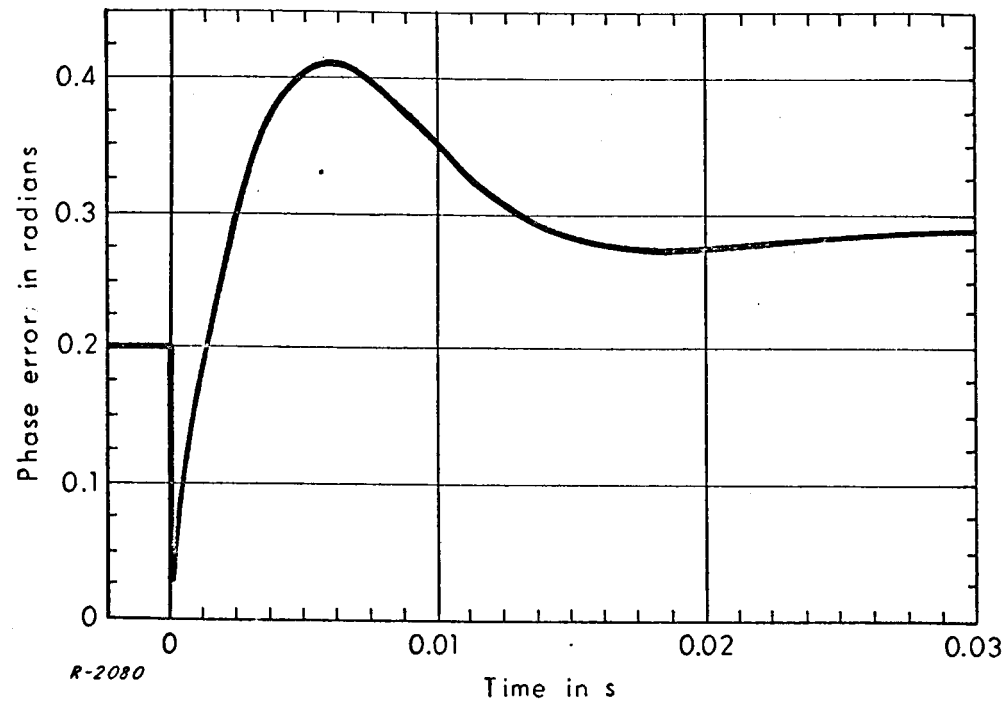

Fig. 3.17a Loop Phase Error, Case I.

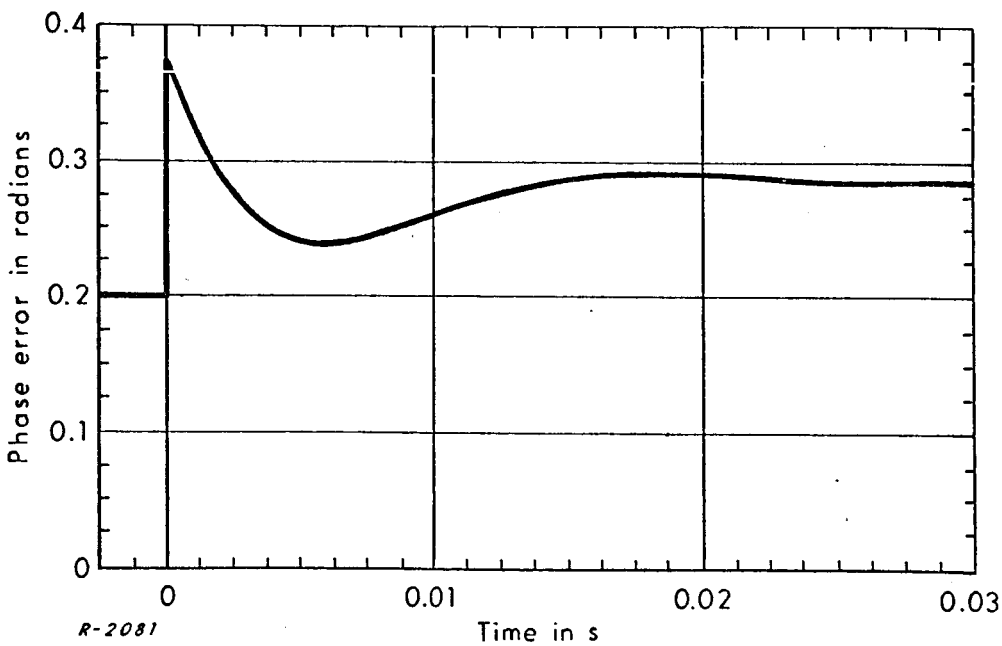

Fig. 3.17b Loop Phase Error, Case II.

is pessimistic. As the AGC loop gain approaches its maximum value the amplitude transient will die out completely within a few milliseconds and the only effect on phase error in the carrier loop will come from the phase step. Under this condition Eq. (3.70) does not apply and the only response required is the phase step response. Equations (3.67)-(3.70) can be used if a is set equal to one, which removes the amplitude dependence.

We may also consider the phase error response with the polarity or direction of the phase step reversed, assuming low AGC loop gain so that Eq. (3.70) may be used. Using the same loop parameters and a = 0.708 as before, yields the response plotted in Fig. 3.17b. Here the peak phase error occurs immediately and is of short duration. In this case the peak is 0.375 radians which is less than in Fig. 3.17a. If the magnitude of the phase step Φ is allowed to increase, the peak phase error values of both cases will increase, but for the curve of Fig. 3.17b its peak error will increase faster. The peak error in the first case is

$$E_1 = \frac{\Omega}{aK} + \left[\frac{(a-1)}{a}\,\frac{\Omega}{K} - |\Phi|\right](-k) \qquad (3.72)$$

where k is the peak value of the overshoot in the unit step response part of $e_s(t)$ and $|\Phi|$ represents a magnitude so the minus sign must appear. The peak error in the second case is

$$E_2 = \frac{\Omega}{aK} + \left[\frac{(a-1)}{a}\,\frac{\Omega}{K} + |\Phi|\right] \qquad (3.73)$$

If these errors are equated, we can solve for the value of the input phase step $|\Phi|_c$ at which the peak errors cross over, viz

$$|\Phi|_c = \frac{1+k}{1-k}\left(\frac{1}{a} - 1\right)\frac{\Omega}{K} \qquad (3.74)$$

Using the previous values of a, Ω, and K and using k = 0.49 we obtain

$$|\Phi|_c = 0.243 \text{ rad} = 14^o \qquad (3.75)$$

For any value of Φ greater than 14^o the response of Fig. 3.17b will show the greatest peak phase error.

4. PERFORMANCE OF THE VTR RANGE LOOP

4.1 Introduction

This section contains analyses relating to the VTR range loop. It essentially consists of two separate analyses. The first and important study is the effect of uplink data on the L-code acquisition. It is shown in this section that uplink data can reduce the correlation level of the code nearly 25%. This means that uplink data reduces the system threshold for acquisition. Conversely, it shows that reliability of low-code acquisition can be kept high if no uplink data is transmitted during low-code acquisition. The second analysis in this Section is that of the combined carrier and range processing scheme used in AROD. First the basic model of the processing used in AROD is derived, and next expressions for variance of the range measurement noise are obtained. Finally, the model used in the analysis by Motorola (Report No. 3065-2-1, Revision 2, 1 September 1965) is compared and the effect of differences in the two models indicated.

4.2 Effect of Uplink Data on L-Code Acquisition*

In the AROD system, the first acquisition step involves correlating the received L-code with a shifting L-code generated by the local code generator on-board the vehicle. If there is no data modulation on the received L-code, the cross-correlation function of these two L-codes is the autocorrelation function of the L-code, shown in Fig. 4.1.

Now let data bits be added modulo to the incoming L-code (denoted by L⊕ data. When the L-component of the incoming signal is in-phase with the local L-code, all the binary digits of these two codes in one L-code period are in-phase except for 8 digits due to the effect of data modulation.

---

* This section was originally presented as ADCOM Technical Memorandum G-69-1 entitled, "The Effect of Uplink Data Transmission on L-Code Acquisition in the AROD System," 6 August 1965.

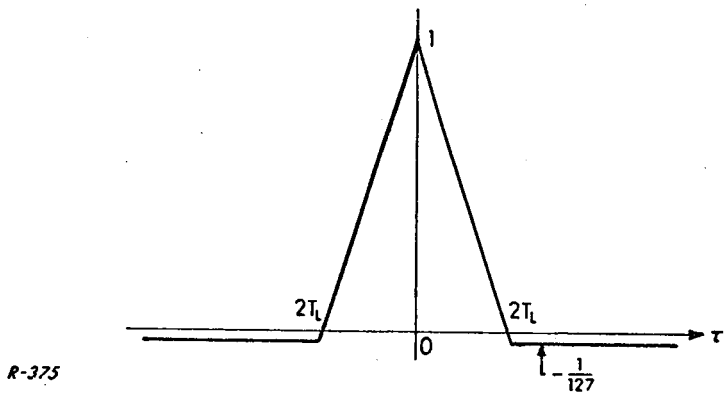

Fig. 4.1 Autocorrelation Function of L-Code.

Each data digit is composed of either a 1010101010101010 or 0101010101010101 pattern of subdigits. Each subdigit has the same bit length as that of an L-code digit, and two adjacent data subdigits are separated by 7 L-code digits. It can be easily seen that all the "zeros" of the data subdigits have no effect on the L-code which is modulated by the data digits, and all the "ones" of the data subdigits will complement the L-code digits, a total of 8 changed bits per L-code period.

Let τ indicate the time shift by which L⊕ data leads the local L-code and $\rho(\tau)$ be the corresponding value of the cross-correlation function.

Then

$$\rho(0) = \frac{127 - (2 \times 8)}{127} = \frac{111}{127} = 0.874 \qquad (4.1)$$

Both L-code and L⊕ data are binary waveforms, hence $\rho(\tau)$ must be a continuous and piecewise linear waveform. The first derivative of $\rho(\tau)$ is discontinuous at $k(2T_L)$, where k is an integer. Therefore, once the points at $k(2T_L)$ are determined, the complete waveform $\rho(\tau)$ is known. The autocorrelation function of the L-code has a value of -1/127 for $\tau = k(2T_L)\, k \neq 0$, which means that $(\text{L-code})_t \oplus (\text{L-code})_{t + k(2T_L)}$ consists of 63 zeros and 64 ones. With data modulation on the received L-code, two extreme cases may occur:

1) All of the 8 "ones" of a data digit within one L-code period change the "ones" of $(\text{L-code})_t \oplus (\text{L-code})_{t+k(2T_L)}$ to "zeros." Hence, $\rho(\tau)$ is bound from above by

$$\frac{(63+8) - (64-8)}{127} = \frac{15}{127} = 0.118 \text{ for } |\tau| \geq 2T_L \qquad (4.2)$$

2) All of the 8 "ones" of a data within one L-code period change the "zeros" of $(\text{L-code})_t \oplus (\text{L-code})_{t+k(2T_L)}$ to "ones." Hence, $\rho(\tau)$ is bound from below by

$$\frac{(63-8) - (64+8)}{127} = -\frac{17}{127} = -0.134 \qquad (4.3)$$

We, then, can visualize the correlation function of L-code and L$\oplus$ data as a triangular wave between $-2T_L \leq \tau \leq 2T_L$ with a peak of 0.874 at $\tau = 0$ and for $|\tau| \geq 2T_L$ the correlation function has a noise-like appearance bounded between 0.118 and -0.134. A cross-correlation function for the data subdigit sequence 1010101010101010 is plotted in Fig. 4.2.

If no data were sent a decision threshold could be set somewhere between -0.00788 and 1. But when up-data is used, the threshold range is confined to the region between 0.118 and 0.874. Therefore, the cross-correlation function with data is equivalent to a triangular function with a peak of 0.874 - 0.118/1 - (-0.00788) = 0.75. Thus the peak of the equivalent correlation function is reduced by 25% due to the data modulation. Under poor signal-to-noise ratio conditions this would be highly undesirable. The only solution then would be to avoid sending up-data till after acquisition.

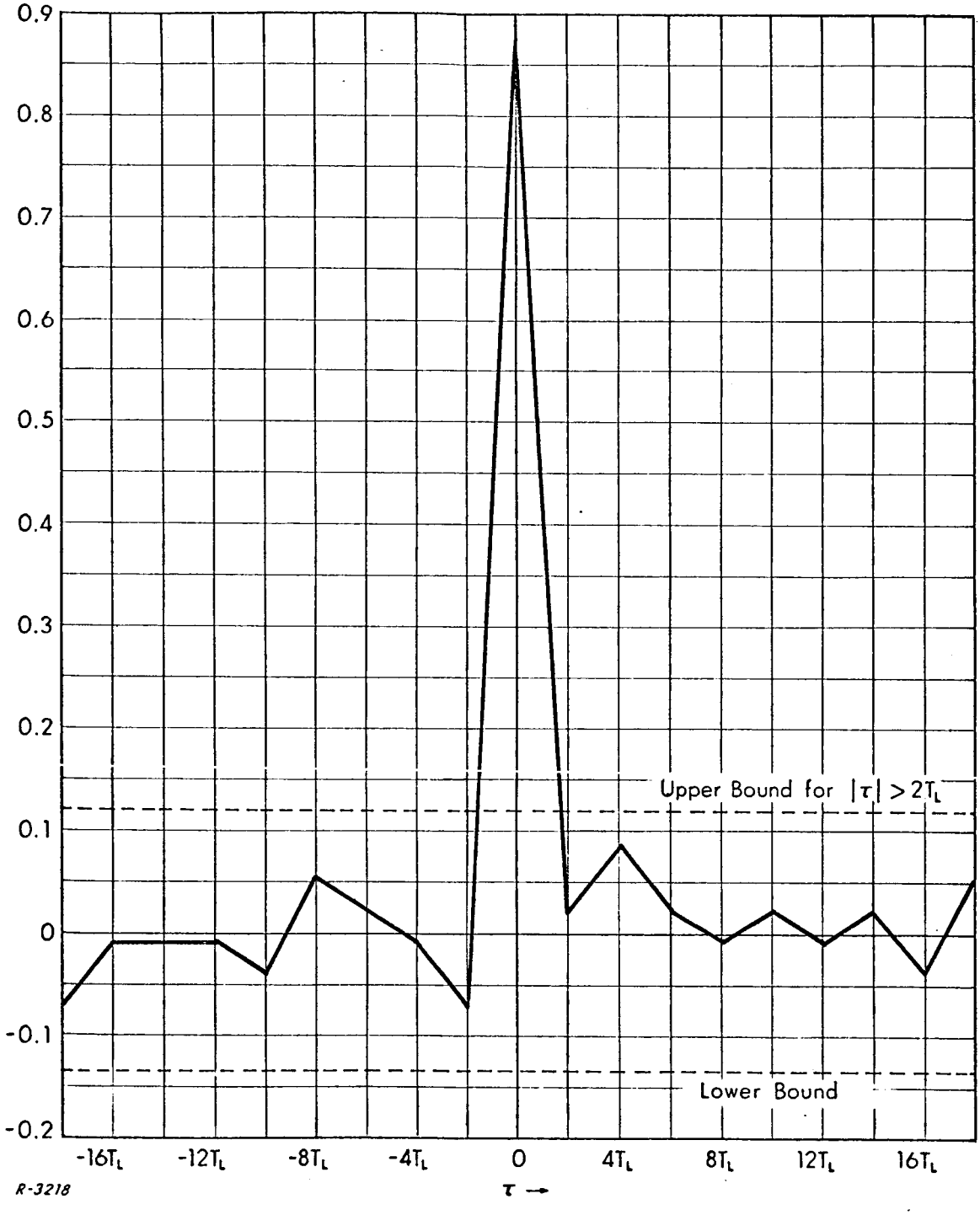

Fig. 4.2 A Cross-Correlation Function of L-Code and L⊕ Data.

4.3 Effect of Cross-Coupled Noise on Range Loop

The combined range and carrier loops of the VTR can be reduced to the block diagram of Fig. 4.3. The standard notation for phase-locked loops is used in this figure. The lowpass filters of the two loops are denoted as $F_m(s)$ and $F_c(s)$. The subscript 'm' for the range modulation and the subscript 'c' for carrier. The phase detector is linearized to a difference, while the difference in the doppler variations of the inputs of the two loops are exactly represented by the ratio of the frequencies ω_c and ω_m. This ratio is about 300. Figure 4.3 shows that essentially the AROD ranging configuration is a rate aiding concept. The problem of this section is then to compute the effects of carrier loop noise introduced into the range loop.

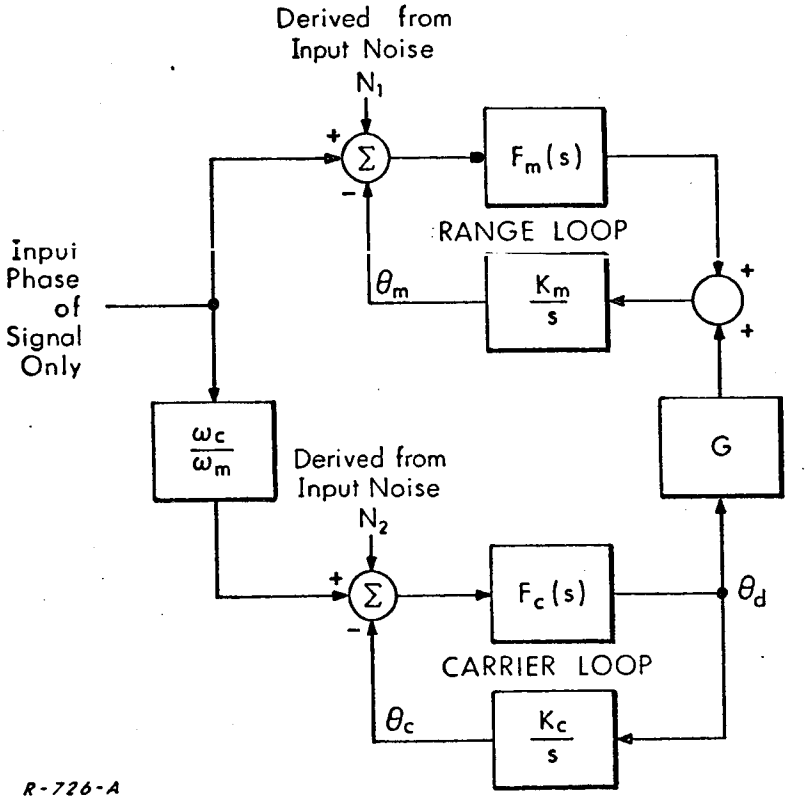

Fig. 4.3 Phase Model of Range and Carrier Loops.

Since the system is linear we can determine the equivalent range loop transfer function and its corresponding noise bandwidth, and consequently the total noise error of the range loop. The inclusion of the gain ω_c/ω_m follows from the fact that the doppler shift of the carrier loop is equal to ω_c/ω_m times that of the range loop.

The carrier loop is assumed to be independent of the range loop. Hence in operational notation

$$\theta_c(s) = \left(\frac{\omega_c}{\omega_m}\right) \frac{K_c F_c(s)}{s + K_c F_c(s)} \theta(s) \tag{4.4}$$

$$\theta_d(s) = F_c(s) \left\{ \frac{\omega_c}{\omega_m} \theta(s) - \theta_c(s) \right\} \tag{4.5}$$

substituting Eq. (4.4)

$$\theta_d(s) = \frac{\omega_c}{\omega_m} \frac{s F_c(s)}{s + K_c F_c(s)} \theta(s) \tag{4.6}$$

Now, for the range loop

$$\theta_m(s) = \frac{K_m}{s} \left[F_m(s) \{\theta(s) - \theta_m(s)\} + G\, \theta_d(s) \right] \tag{4.7}$$

or

$$\frac{1 + K_m F_m(s)}{s} \theta_m(s) = \frac{K_m F_m(s)}{s} \theta(s) + \frac{K_m G}{s} \theta_d(s) \tag{4.8}$$

therefore

$$\theta_m(s) = \frac{K_m F_m(s)}{s + K_m F_m(s)} \theta(s) + \frac{K_m G}{s + K_m F_m(s)} \theta_d(s) \tag{4.9}$$

substituting Eq. (4.6)

$$= \left[F_m(s) + \frac{\omega_c}{\omega_m} \frac{s G F_c(s)}{s + K_c F_c(s)} \right] \frac{K_m}{s + K_m F_m(s)} \theta(s) \qquad (4.10)$$

Denoting the transfer functions to the input phase of the range loop and carrier loop as

$$Y_m(s) = \frac{K_m F_m(s)}{s + K_m F_m(s)} \; ; \; Y_c \frac{K_c F_c(s)}{s - K_c F_c(s)} \qquad (4.11)$$

since $\{1 - Y_m(s)\} = \frac{s}{s + K_m F_m(s)}$ we can write

$$\theta_m(s) = \left[Y_m(s) + G\left(\frac{K_m}{K_c}\right)\left(\frac{\omega_c}{\omega_m}\right) \left(1 - Y_m(s)\right) Y_c(s) \right] \theta(s) \qquad (4.12)$$

and

$$\frac{\theta_m(s)}{\theta(s)} = Y_m(s) + G\left(\frac{K_m}{K_c}\right)\left(\frac{\omega_c}{\omega_m}\right)\left(1 - Y_m(s)\right) Y_c(s) \qquad (4.13)$$

The noise processes N_1 and N_2 shown in Fig. 4.3 are statistically independent, and their equivalent input noise power spectral densities Φ_{N1} and Φ_{N2} are essentially white and related as follows

$$\Phi_{N1} = \frac{N_o}{2A^2} \quad \text{(range loop noise input)} \qquad (4.14)$$

$$\Phi_{N2} = \frac{N_o}{2A^2} \cdot \left(\frac{\omega_m}{\omega_c}\right)^2 \quad \text{(carrier loop noise input)} \qquad (4.15)$$

Since $B_m \ll B_c$, the output phase noise power of the range loop is approximately

$$\sigma_n^2 = \frac{\pi N_o}{A^2} \left\{ B_m + \left(\frac{K_m G}{K_c} \right)^2 \left(B_c - B_m \right) \right\} \text{ (rad)}^2 \tag{4.16}$$

For ideal rate aiding,

$$\frac{K_m G}{K_c} = \frac{\omega_m}{\omega_c} \tag{4.17}$$

therefore

$$\sigma_n^2 = \frac{\pi N_o}{A^2} \left\{ B_m + \left(\frac{\omega_m}{\omega_c} \right)^2 \left(B_c - B_m \right) \right\} \tag{4.18}$$

If the rate aiding is not perfect, for example a 10% variation of the gain G is allowed, then the mean-square value of the output phase noise of the range loop is

$$\sigma_n^2 = \frac{\pi N_o}{A^2} \left\{ B_m + (1 \pm 0.1)^2 \left(\frac{\omega_m}{\omega_c} \right)^2 \left(B_c - B_m \right) \right\} \tag{4.19}$$

Since $\left(\frac{\omega_m}{\omega_c} \right)^2$ is very small, the additional noise due to the rate aiding is small enough to be tolerable. Let us now determine the bandwidth B_{mo} required to keep the range loop dynamic error the same, if the rate aiding is not 100%. Define the error

$$\epsilon(s) = \theta(s) - \theta_m(s) \tag{4.20}$$

Then,

$$\epsilon(s) = \theta(s) - \left[Y_m(s) + G\left(\frac{K_m}{K_c}\right)\left(\frac{\omega_c}{\omega_m}\right)Y_c(s)\right]\theta(s) \qquad (4.21)$$

$$= \left(1 - Y_m(s)\right)\left[1 - G\left(\frac{K_m}{K_c}\right)\left(\frac{\omega_c}{\omega_m}\right)Y_c(s)\right]\theta(s) \qquad (4.22)$$

Let $G\left(\frac{K_m}{K_c}\right)\left(\frac{\omega_c}{\omega_m}\right) = 1 - \delta$, where δ is the fractional inaccuracy in rate aiding it is a small quantity. Thus Eq. (4.22) becomes

$$\epsilon(s) = \left(1 - Y_m(s)\right)\left[1 - (1-\delta)\,Y_c\right]\theta(s) \qquad (4.23)$$

Define

$$E_m(s) = 1 - Y_m(s) \text{ and } E_c(s) = 1 - Y_c(s) \qquad (4.24)$$

Therefore

$$\epsilon(s) = E_m(s)\left[\delta + (1-\delta)\,E_c(s)\right]\theta(s) \qquad (4.25)$$

$$= \delta E_m(s)\,\theta(s) + (1-\delta)\,E_m(s)\,E_c(s)\,\theta(s) \qquad (4.26)$$

The velocity gain constant of the carrier loop is high resulting in a small $E_c(s)$ for all the frequencies under consideration. Hence,we can approximate

$$\epsilon(s) \approx \delta E_m(s)\,\theta(s) \qquad (4.27)$$

Thus if δ is zero, i.e., perfect rate aid, we see that the dynamic error of the range loop is zero. On the other hand, if a range loop was designed without any rate aiding, its dynamic error is given by

$$\epsilon_o(s) = E_{mo}(s)\,\theta(s) \qquad (4.28)$$

where the subscript 0 is used to indicate that transfer functions $Y_m(s)$ and $E_m(s)$ will be different for a range loop not employing rate aiding. Comparing Eqs. (4.22) and (4.23), we can show that for the same dynamic error the noise bandwidths of two loops, one employing rate aiding and the other no rate aiding, are related by

$$B_{mo} = \frac{B_m}{\sqrt{\delta}} \tag{4.29}$$

where δ is the fractional accuracy of the rate aid. This is an interesting relation. First of all, it recognizes that rate aiding cannot be perfect; secondly, it shows the considerable reduction in noise bandwidth of the range loop, since $\delta \ll 1$.

It will be noted that the above analysis, and in particular the final expression for σ_n^2 (see Eq. (4.19)), differs from that of Sec. 3.5, Ref. 1. The difference in σ_n^2, however, is only in the second term, which was found to be small. The expression of Eq. (4.24) remains the same for both the model of Fig. 4.3 and that of Fig. 3.28 in Ref. 1

5. NOISE ANALYSIS OF VTR'S COHERENT AGC*

5.1 Introduction

In the Vehicle Tracking Receiver coherent AGC is employed to maintain the signal levels into the phase detectors of the carrier and range loops as nearly constant as possible when the signal level into the first mixer of the tracking subsection is higher than -85 dBm as shown in Fig. 5.1. The limiter after the gain-controlled IF amplifier functions as a linear amplifier provided the input signal exceeds -85 dBm and the AGC loop operates properly. Since there is no limiting at these signal levels any noise due to AGC passes on to phase detectors. The object of this section is to estimate this noise effect.

Since the coherent AGC only operates after the low-code is acquired, the existence of the balanced demodulator which correlates the incoming range modulation with the range loop output is simply to remove the range modulation. Thus the analysis of the AGC performance of the combined carrier and range loop can be done as a simple carrier loop.

5.2 IF Amplitude Jitter Due to Carrier PLL Phase Jitter

The carrier loop output is mixed with the incoming signal from the balanced demodulator before it is fed into the gain-controlled IF amplifier. The carrier loop error will change the effective signal amplitude into the IF amplifier since the carrier loop output is a sinusoidal wave.

Let $\sqrt{2}A$ denote the amplitude of the input signal and let $\Phi(0)$ be the power density of the input noise which is assumed to be white and Gaussian.

---

* This material was originally presented as ADCOM Technical Memorandum G-69-6, entitled, "A Consideration Concerning the AGC Loop Performance," 16 December 1965.

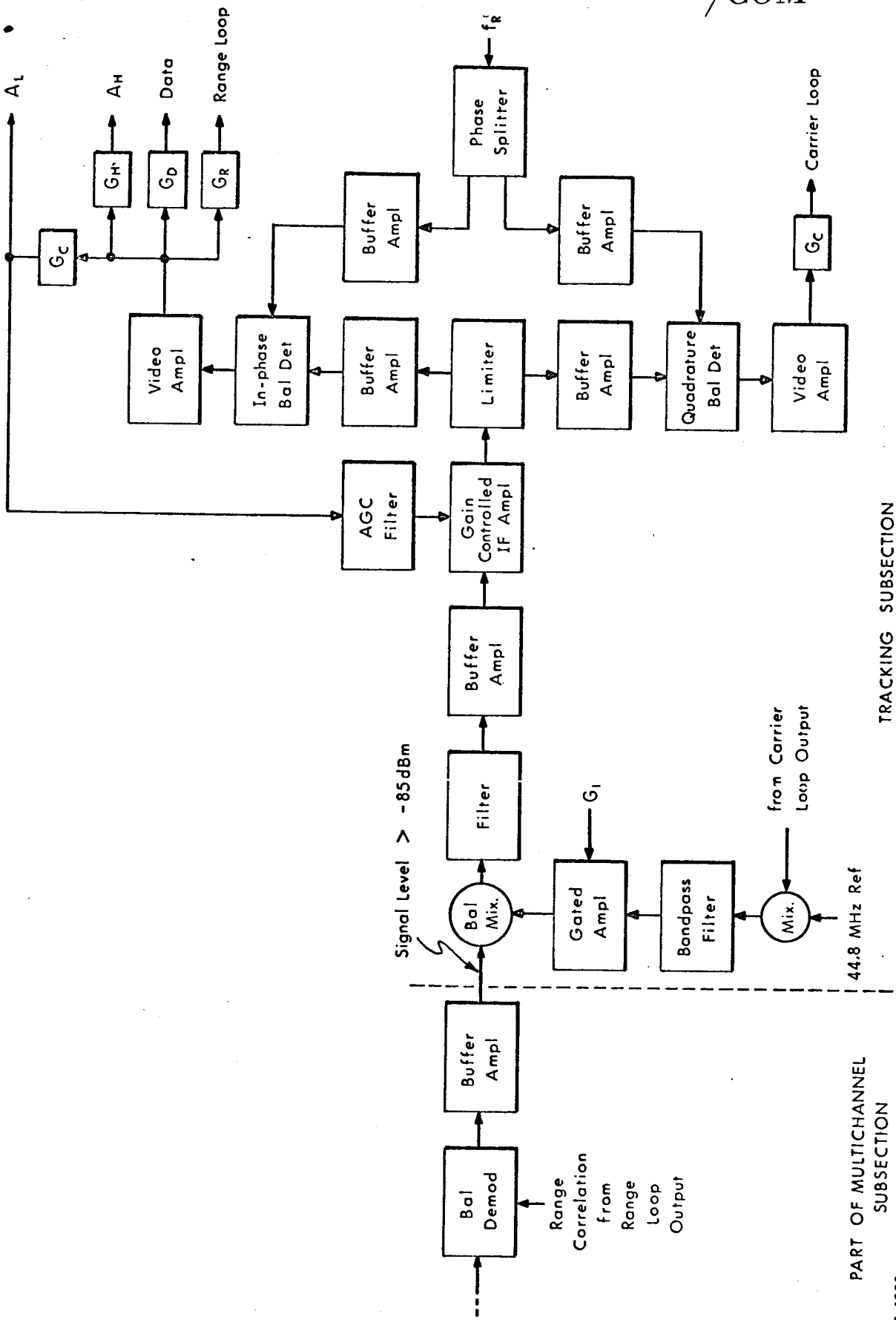

Fig. 5.1 Part of Vehicle Tracking Receiver of the AROD System.

Define $N = \frac{\Phi(0)}{A^2}$, the normalized power density of the input noise in Hz^{-1}.

If the gain of the IF amplifier is assumed to be constant, then the carrier loop output phase error ϵ_c is also Gaussian since in this case the PLL can be considered as a linear loop. The Gaussian process is characterized by the following two parameters.

$$\overline{\epsilon_c} = 0 \tag{5.1}$$

and

$$\overline{\epsilon_c^2} = NB_{nc} \tag{5.2}$$

where B_{nc} is the two-sided noise bandwidth of the carrier loop. The probability density function is:

$$p(\epsilon_c) = \frac{1}{\sqrt{2\pi NB_{nc}}} e^{-\frac{\epsilon_c^2}{2NB_{nc}}} \tag{5.3}$$

The moments of ϵ_c are:

$$\overline{\epsilon_c^{2n+1}} = 0, \quad n = 0,1,2,3,\ldots$$

$$\overline{\epsilon^{2n}} = 1.3.5\ldots(2^n-1)\,(\overline{\epsilon^2})^n, \quad n = 1,2,3,\ldots \tag{5.4}$$

or

$$\overline{\epsilon^{2n}} = 1.3.5\ldots(2^n-1)\,(NB_{nc})^n \tag{5.5}$$

The input amplitude of the gain-controlled IF amplifier can be expressed as

$$A \cos \epsilon_c \approx A\left(1 - \frac{\epsilon_c^2}{2}\right) \text{ since usually } \epsilon_c \ll 1 \text{ rad} \qquad (5.6)$$

Normalized by A, the input amplitude of the IF is $1 - \frac{\epsilon_c^2}{2}$, and we can consider the first term as the desired amplitude and the second term as the extra noise caused by the interference of the carrier loop. Let $n_c = \frac{\epsilon_c^2}{2}$ the probability density function of n_c can be obtained by

$$p(n_c) = 2p(\epsilon_c) \left| \frac{d\epsilon_c}{dn_c} \right| \qquad (5.7)$$

The factor 2 comes from the fact that both $-\epsilon_c$ and $+\epsilon_c$ are mapped into the same n_c. Evaluating (5.7) we have:

$$p(n_c) = \begin{cases} \dfrac{1}{\sqrt{\pi N B_{nc} n_c}} e^{-\frac{n_c}{NB_{nc}}} & , \ n_c > 0 \\ 0 & , \ n_c < 0 \end{cases} \qquad (5.8)$$

$$\overline{n_c} = \frac{\epsilon_c^2}{2} = \frac{1}{2} NB_{nc} \qquad (5.9)$$

$$\overline{n_c^2} = \overline{\left(\frac{\epsilon_c^2}{2}\right)^2} = \frac{1}{4} \overline{\epsilon_c^4} = \frac{3}{4} (NB_{nc})^2 \qquad (5.10)$$

The results of (5.9) and (5.10) are obtained from (5.5). The variance of n_c is then given by

$$\sigma^2_{n_c} = \overline{n_c^2} - \overline{n_c}^2 = \frac{1}{2}(NB_{nc})^2 \qquad (5.11)$$

and the standard deviation is

$$\sigma_{n_c} = \frac{1}{\sqrt{2}} NB_{nc} \qquad (5.12)$$

5.3 Total Effects of Coherent AGC

The effect of the AGC can be determined through use of a linear model of the AGC loop[4] which is valid over any small range of input level variations. The linear model requires the amplifier gain control characteristic, expressed as the logarithm of the gain versus the control voltage, to be linear. It also requires the AGC detector gain control in volts/dB change in amplifier output level to be constant.

The filter in the AGC loop has the transfer function

$$Y(s) = \frac{1}{1 + \tau s} \qquad (5.13)$$

where τ is the time constant of the filter. Since the gate G_c closes for one-quarter of the time, it is required that the time constant τ should be much longer than 0.16 ms, the time interval that the gate G_c is open so that the AGC gain can be held constant all the time independent of closing or opening of the gate G_c.

The closed-loop transfer function of the AGC loop is

$$H(s) = \frac{1}{\left(1+\frac{1}{G}\right)+\frac{\tau}{G}s} \tag{5.14}$$

where G is the open-loop AGC gain in dB change in amplifier gain per dB change in amplifier output. The noise bandwidth of the AGC loop in Hz is

$$B_{AGC} = \frac{1}{2\pi}\int_{-\infty}^{\infty} |H(j\omega)|^2 \, d\omega = \frac{\frac{G}{2\tau}}{1+\frac{1}{G}} \tag{5.15}$$

A PLL phase model can be considered as a lowpass filter, hence the phase error ϵ_c of the carrier loop output contains no high frequency components $n_c = \frac{\epsilon_c}{2}$ is also a low-frequency random variable since it can be obtained by doubling ϵ_c frequency. Therefore, it is safe to assume that the AGC loop output due to n_c is approximately given by

$$V_{n_c} = \sigma_{n_c} \cdot |H(0)| = \frac{1}{\sqrt{2}} NB_{nc} \cdot \left|\frac{1}{1+\frac{1}{G}}\right| = \frac{\frac{1}{\sqrt{2}}NB_{nc}}{1+\frac{1}{G}} \tag{5.16}$$

The AGC output is also affected directly by the noise N:

$$V_N^2 = N \cdot B_{AGC} = \frac{\frac{NG}{2\tau}}{1+\frac{1}{G}} \tag{5.17}$$

From (5.16) and (5.17), a measure of the gain variations of the IF amplifier can be estimated from the expression

$$G_{IF} = \frac{1}{1 \pm V_{n_c} \pm V_N} \approx 1 \mp V_{nc} \mp V_N$$

$$\approx 1 \mp \frac{\frac{1}{\sqrt{2}} NB_{nc}}{1 + \frac{1}{G}} \mp \sqrt{\frac{\frac{NG}{2\tau}}{1 + \frac{1}{G}}} \qquad (5.18)$$

The carrier loop noise bandwidth B_{nc} = 400 Hz. Let us assume the time constant of the AGC loop filter τ = 1 s, and G≈50. When the input signal level is -85 dBm it can be shown that $N = 2.45 \times 10^{-5}$ Hz $^{-1}$. Substituting these values into (5.18), we see that G_{IF} varies ±0.025 about 1. In this case, the term V_{nc} contributes approximately one-quarter to the fluctuation of G_{IF} and the other three-quarters is attributed to V_N. This AGC effect may be looked at as slight amplitude modulation by noise of the IF amplifier input. As the signal level increases this noise will decrease, while for low signal-to-noise ratios the limiter would remove the amplitude noise, although simultaneously suppressing the signal and hence reducing the carrier phase-locked loop bandwidth.

REFERENCES

1. Motorola, Inc., Military Electronics Division, "AROD System Description," Report No. 3065-2-1, Prepared for MSFC, Contract No. NAS8-11835, Revisions 1, 2, 3, 4 from 4 June 1965 to 1 March 1966.

2. Kline, A.J., "AROD Vehicle Tracking Receiver Design," Technical Memorandum No. 3065-26, 3 August 1966, Government Electronics Division, Aerospace Center, Motorola, Inc.

3. Kruse, K.W. and Meer, S.A., "Study of the Goddard Range and Range Rate System for the Applications Technological Satellite," Final Report on Contract No. NAS5-3694, ADCOM, Inc., 1 May 1965.

4. Victor, W.K. and Brockman, M.H., "The Application of Linear Servo Theory to the Design of AGC Loops," Proc. IRE, pp. 234-238, February 1960.